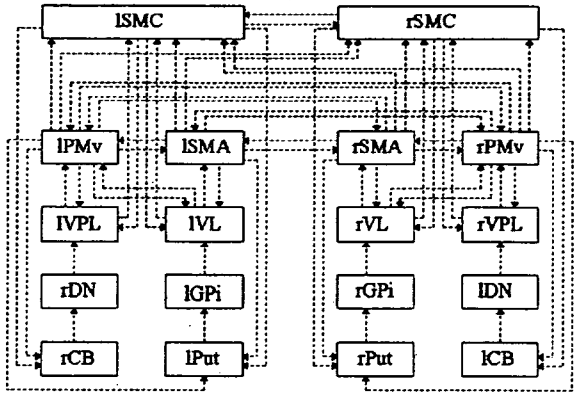

Fig. 1. A diagram illustrating the major cortical and subcortical structures involved in the sequential finger movements of SI and ET tasks, and their interconnections. These structures are organized into a basal ganglia–thalamo–motor loop, a cerebello-cerebral loop and connectivity within motor cortices. *Abbreviations:* Put, putamen; GPi, internal segment of the globus pallidus; VL, ventrolateral nucleus of the thalamus; VPL, ventro–posterior–lateral nucleus and X area of the thalamus; SMA, supplementary motor area; SMC, primary sensory-motor cortex; PMv, ventral premotor cortex; CB, cerebellar hemisphere (anterior lobe); DN, dentate nucleus of the cerebellum. r=right, l=left in this and subsequent figures.

no significant pathological change was found by anatomical T1- and T2-weighted MRI, although there were some changes due to normal aging. All subjects were strongly right-handed as assessed by a modified version of the Edinburgh handedness inventory (Oldfield, 1971). Informed written consent was obtained from all subjects for participation in this study. The local ethical committee of Kyushu University approved this study.

Experimental design

The activation paradigm consisted of sequential movements performed with the left hand as previously described (Taniwaki et al., 2003; 2006). We intended to reveal the movement-rate-related activity but not simple repetitive or externally cued movements. From our previous study (Taniwaki et al., 2003; 2006), sequential or internally cued movement could indicate movement-rate-related activity of the basal ganglia. Non-dominant hand movements cause a greater recruitment of the striatum (Mattay et al., 1998) and cerebellum (Jancke et al., 1999). Thus, we used sequential finger movements in the left hand.

Subjects were instructed to move each finger with changing movement rates. They were then required to practice the tasks before they were scanned, until they were able to perform them at constant amplitude without error. They were also instructed to keep their eyes

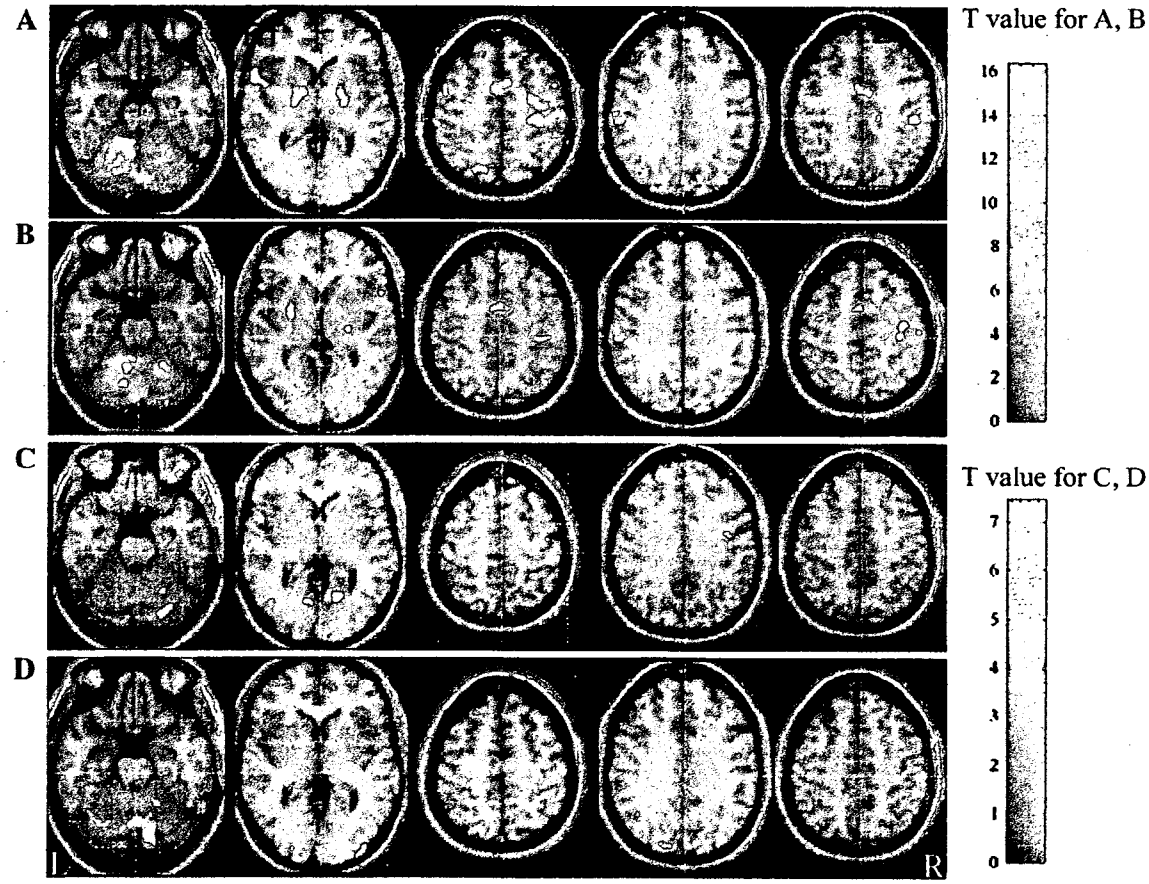

Fig. 2. Regions showing main effects of movement rate (A and B) and significant linear relationship between BOLD signal and increasing movement rate (C and D) in the aged group. All regions are significant at the level of $p<0.001$, uncorrected. A, C: self-initiated movements; B, D: externally triggered movements in this and subsequent figures.

closed during MRI. Subjects had to (1) make finger-to-thumb opposition movements in the order of index, middle, ring and little fingers; (2) open and clench the fist twice; (3) complete finger-to-thumb opposition movements in the opposite order (namely, little, third, middle and index fingers); (4) once again open and clench the fist twice; and (5) repeat the same series of movements for 40 s during data acquisition. Each individual opposition movement and pair of opening and clenching fist movement was counted as a single movement. During SI tasks, movement rates were set at very slow (as slow as possible), slow, moderate (comfortable pace), fast and very fast (as fast as possible) speeds. During ET tasks, movement rates were set at 0.5, 1, 2, 3 or 4 Hz for all subjects. Subjects paced their movements in response to a metronome, which consisted of a clicking sound at precise time intervals and was delivered binaurally to the subjects via air conduction through a pair of 2.5-m long plastic tubes. During rest conditions, subjects were asked to lie down and listen to the metronome used in the ET session. Movements were performed for 40 s (activation) at a constant rate, followed by 40 s of rest (baseline); the time-point to switch from movement to rest was indicated by a voice signal. Movement rate conditions were presented in a pseudorandom order within an imaging series. Consequently, there were a total of five baseline/activation cycles (for the five different rates) per imaging series. Two consecutive imaging series (one SI, and one ET) were conducted per subject. The order of SI and ET movements was counter-balanced among the subjects. Finger movements were recorded by digital video recording, and exact movement rates were analyzed visually through a video monitor. Two-way analysis of variance (ANOVA) with repeated measures was performed to determine effects of movement rates and tasks.

fMRI methods

Images were acquired on a 1.5 T Magnetom SYMPHONY (Siemens, Enlangen, Germany) whole body MRI system equipped with a circular polarized volume head coil, as previously described (Taniwaki et al., 2003; 2006). Initially, a set of localized images was acquired to position the image slice. In each session, 100 EPI multislice data sets were acquired (TE, 50 ms; TR, 4 s, flip angle, 90°; acquisition time for the whole paradigm, 400 s). Each multislice data set contained 32 transverse slices (slice thickness, 3.0 mm; interslice gap, 1.0 mm; matrix, 64 × 64; FOV, 23 cm). All images were analyzed using SPM 2 Software (Wellcome Department of Cognitive Neurology, London, UK). The first three data sets of each time-series were discarded in order to allow the MRI signal to reach equilibrium, and the remaining EPI volumes were realigned against the first volume. Images were spatially normalized against a standard template and smoothed using a Gaussian kernel with 8-mm full width at half maximum (FWHM). The design matrix was set using the box car reference waveform (40-s epoch). The time-series in each voxel was high-pass filtered (160-s cut-off) and scaled to a grand mean of 100 over voxels and scans within each session.

Activation areas

Activation areas were determined as previously described (Taniwaki et al., 2006). In brief, statistical analysis was performed in two stages. In the first stage, using a single subject fixed effect model and parametric approach in SPM 2, three different rate–response relationships could be identified: (1) categorical on–off responses based on the differences between finger movement and resting conditions regardless of movement rates (zero order term), (2) linear responses in parallel with movement rate (first-order term), and (3) non-linear relationship (second, third and fourth order term) (Büchel et al., 1996, 1998). Each term was represented by the interaction between a delta function and the average of movement rates exerted during each epoch. The resulting covariates were convolved with a canonical synthetic hemodynamic response function and were used in a general linear model (Friston et al., 1995), together with a single covariate representing the mean (constant) term over scans. Parameter estimates for each covariate resulting from the least mean squares fit of the model to the data were calculated, and statistical parametric maps of the *t*-statistic (SPM{*t*}), resulting from linear contrasts of each covariate (Friston et al., 1995), were generated and stored as separate images for each subject.

Table 2
Brain areas with more activation in aged subjects than in young subjects

	Main effect				Linear effect			
	Coordinates				Coordinates			
	Z	*x*	*y*	*z*	*Z*	*x*	*y*	*z*
SI movement								
rPut	n.s.				n.s.			
rGPi	n.s.				n.s.			
rVL	n.s.				n.s.			
rVPL	n.s.				n.s.			
rSMA	n.s.				n.s.			
rSMC	n.s.				n.s.			
rPMv	n.s.				n.s.			
lCB	n.s.				n.s.			
lDN	n.s.				n.s.			
lPut	n.s.				n.s.			
lGPi	n.s.				n.s.			
lVL	n.s.				n.s.			
lVPL	n.s.				n.s.			
lSMA	n.s.				n.s.			
lSMC	3.89	−52	−16	54	n.s.			
lPMv	n.s.				n.s.			
rCB	n.s.				n.s.			
rDN	n.s.				n.s.			
ET movement								
rPut	n.s.				n.s.			
rGPi	n.s.				n.s.			
rVL	n.s.				n.s.			
rVPL	n.s.				n.s.			
rSMA	n.s.				n.s.			
rSMC	n.s.				n.s.			
rPMv	n.s.				n.s.			
lCB	n.s.				n.s.			
lDN	n.s.				n.s.			
lPut	n.s.				n.s.			
lGPi	n.s.				n.s.			
lVL	n.s.				n.s.			
lVPL	n.s.				n.s.			
lSMA	4.08	−10	−18	40	n.s.			
lSMC	4.83	−32	−24	56	n.s.			
lPMv	n.s.				n.s.			
rCB	n.s.				n.s.			
rDN	n.s.				n.s.			

Z-values refer to activation maxima within the respective region, $p < 0.001$ uncorrected, height threshold $Z > 3.09$.

In order to create activation maps representing the main effects of movement rates (0th order), as well as the linear (1st order) and non-linear (2nd, 3rd and 4th order) changes in signals in relation to movement rates, random-effect analysis was performed (Friston et al., 1999). Data for the second stage of analysis comprised pooled parameter estimates for each covariate across all subjects. Contrast images for each subject were entered into a one-sample t-test for each covariate of interest. The SPM$\{t\}$ values were thresholded at $p<0.001$ for mapping. For the comparison of activation between the young and aged group, a two-sample t-test model ($p<0.001$) was used. Anatomical labels for coordinates in SPM2 (MNI brain template) were defined by Talairach Daemon (http://ric.uthscsa.edu/projects/talairachdaemon.html) after a non-linear transformation of the MNI brain template to the Talairach atlas (http://www.mrc-cbu.cam.ac.uk/Imaging/Common/mnispace.shtml). For SEM, ROIs were selected at the local maxima from the first-order linear effect regardless of the tasks (Taniwaki et al., 2006). Therefore, we investigated the following regions with the following coordinates in young subjects: right putamen (Put) (28, −6, 0), right internal segment of the globus pallidus (GPi) (10, −2, −2), right ventrolateral nucleus of the thalamus (VL) (16, −14, 16), right ventro–posterior–lateral nucleus of the thalamus (VPL) (18, −22, 6), right supplementary motor area (SMA) (6, −2, 40), right sensorimotor cortex (SMC) (48, −20, 52), right ventral premotor cortex (PMv) (52, 2, 38), right dentate nucleus of the cerebellum (DN) (18, −54, −22), right anterior lobe of cerebellar hemisphere (CB) (26, −56, −26), and left Put (−26, −14, 4), left GPi (−12, 0, 0), left VL (−12, −12, 12), left VPL (−12, −20, 8), left SMA (−6, 0, 42), left SMC (−40, −18, 58), left PMv (−56, 0, 32), left DN (−22, −50, −22) and left CB (−30, −54, −22). In aged subjects, some coordinates were also selected at the local maxima from the subjects' first-order linear effect regardless of the tasks: right SMA (2, −4, 48), right SMC (42, −12, 54), right PMv (40, −8, 40), right DN (16, −52, −20), right CB (36, −66, −18), and left VPL (−22, −18, 12), left SMC (−50, −12, 44), left PMv (−56, −8, 38), left DN (−8, −54, −22) and left CB (−26, −68, −16). Other ROIs were selected from the same coordinates in young subjects.

Structural equation modeling

In this analysis, variables were considered in terms of the covariance structure with parameters (interregional connection) being estimated by minimizing the differences between observed covariance and those implied by a predicted model. The model consisted of anatomically separable regions, and connections were specified between those regions and their directions. Anatomical

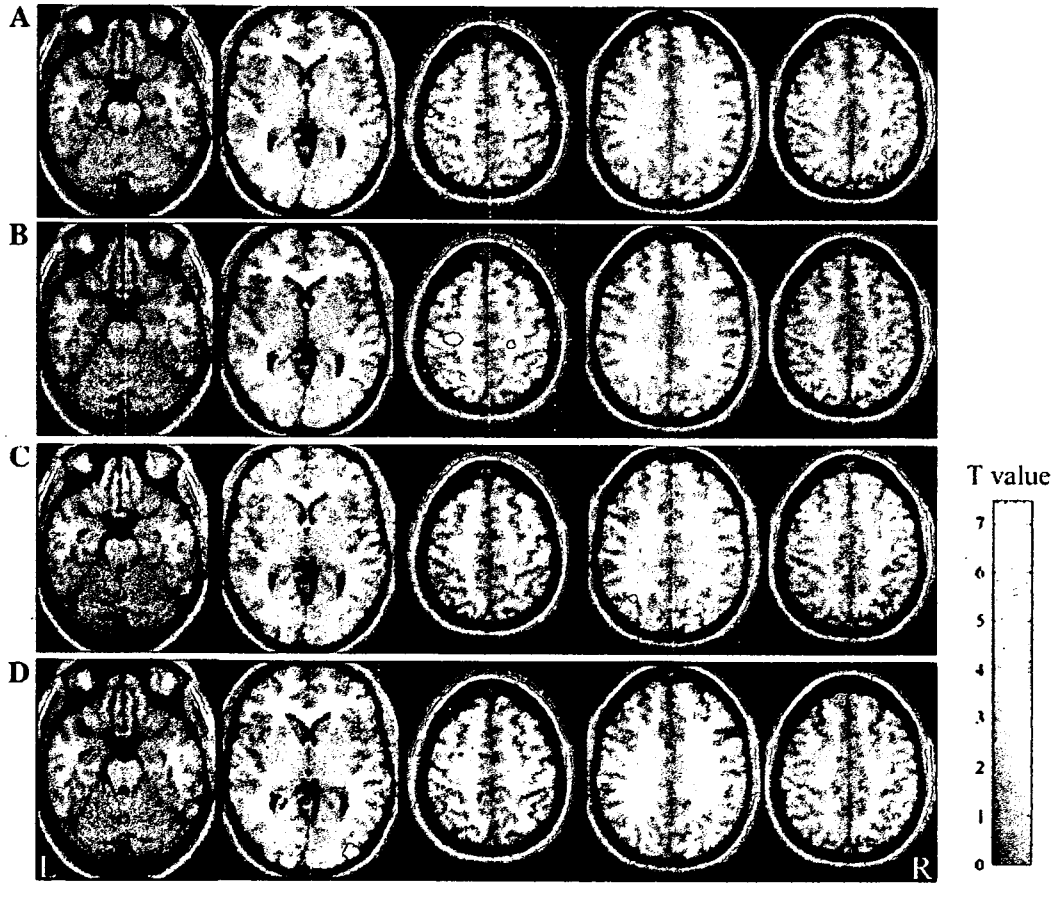

Fig. 3. Brain areas with more activation in aged subjects than in young subjects. Regions showing main effects of movement rate (A and B) and a significant linear relationship between BOLD signal and increasing movement rate (C and D). All regions are significant at the level of $p<0.001$, uncorrected.

regions comprised Put, GPi, VL, VPL, SMA, SMC, PMv, CB and DN (Table 1). Connections between brain regions are based on the neuroanatomical knowledge of BGTM and CC loops (Alexander et al., 1990; Delong, 1990; Kelly and Strick, 2003) as described previously (Taniwaki et al., 2006). The basal ganglia–thalamo–motor (BGTM) loop comprises some cortical motor areas, including the SMA, PMv and SMC, and several subcortical structures such as the Put, GPi and VL. The Put is the input nucleus of the basal ganglia and receives projections from SMA, PMv and SMC. The GPi receives input from the Put and is considered to be an output nucleus of the basal ganglia. In turn, the VL receives projections from the GPi and completes the circuit by projecting back to the SMA, PMv and SMC (Alexander et al., 1990; Delong, 1990). In the cerebello-cerebral (CC) loop, motor cortices such as SMC or PMv are target structures of outputs from the CB via the DN and VPL, while cerebellar inputs originate from these motor cortices (Kelly and Strick, 2003). Between the two loops, SMA and PMv have reciprocal interconnections with each other and project to SMC (Barbas and Pandya, 1987; Johnson et al., 1996; Muakkassa and Strick, 1979; Rizzolatti et al., 1998; Rowe et al., 2002). Recursive connections from the cortex back to the thalamus have also been documented in such a model (Delong, 1990; Grafton et al., 1994). Since significant linear effects were observed in bilateral hemispheres, it was decided to construct an anatomical network for bilateral loops. Interhemispheric connections were constructed by a primate study within motor cortices, such as the SMC, PMv and SMA (Rouiller et al., 1994). A schematic representation of all of the connections used in this study is shown in Fig. 1.

fMRI signal changes were calculated using a single subject fixed effect model. Averaged signal changes of baseline epochs were subtracted from those of each task condition. fMRI data of local maxima in each ROI were standardized to zero mean and to unit variance for each participant (Bullmore et al., 2000; Kondo et al., 2004). The individual time-series for each location were then concatenated into a group matrix for path analysis and subsequent group comparisons ($n=1164$) to obtain stable SEM model solutions. Interregional correlations of activity between selected regions were obtained and the pairwise correlations c_{ij} for the ith and jth regions constituted the $(p \times p)$ interregional correlation matrix. The matrix was combined with a neuroanatomical model (Fig. 1) to compute structural equation models using LISREL 8.5 software (Scientific Software International, Inc, Lincolnwood, IL). A maximum likelihood algorithm was used to fit the parameters. Within-hemisphere functional networks were constructed at first, and the functional network accounting for interhemispheric interactions was calculated in the final stage (McIntosh et al., 1994). The influence of other connections could be estimated by modification indices (McIntosh and Gonzalez-Lima, 1994; McIntosh et al., 1994). Residual influences were set to 0.30 for all regions. Statistical inferences from group differences were based on a stacked model approach including an omnibus test. This procedure determined the χ^2 goodness-of-fit statistic for both a null model, in which path coefficients are equally constrained between conditions, and an alternative model, in which coefficients are allowed to differ (McIntosh et al., 1994). The significance of differences between the models was expressed as the difference in the χ^2 statistic with degrees of freedom equal to differences in the degrees of freedom for the null model and alternative models (McIntosh et al., 1994).

Results

Performance of subjects

During SI movements in aged subjects, very slow movements were performed at a frequency of 1.00±0.37 Hz (mean±SD), slow movements were performed at a rate of 1.26±0.46 Hz, moderate movements were performed at 1.75±0.59 Hz, fast movements were performed at 2.87±0.53 Hz, and very fast movements were performed at 3.43±0.63 Hz. ET movement rates were almost identical to the rates of the auditory triggers (0.5 Hz trigger, 0.56±0.14 Hz; 1 Hz trigger, 0.98±0.04 Hz; 2 Hz trigger, 1.98±0.04 Hz; 3 Hz trigger, 2.94±0.09 Hz; 4 Hz trigger, 3.78±0.16 Hz). In our previous reports of young subjects (Taniwaki et al., 2006), very slow movements were performed at a frequency of

Table 3
Brain areas with more activation in young subjects than in aged subjects

	Main effect				Linear effect			
	Coordinates				Coordinates			
	Z	*x*	*y*	*z*	*Z*	*x*	*y*	*z*
SI movement								
rPut	n.s.				4.19	26	−8	−2
rGPi	n.s.				n.s.			
rVL	n.s.				3.18	8	−14	2
rVPL	n.s.				4.02	16	−22	6
rSMA	n.s.				3.22	4	−2	42
rSMC	3.55	56	−18	46	n.s.			
rPMv	n.s.				n.s.			
lCB	n.s.				n.s.			
lDN	n.s.				n.s.			
lPut	n.s.				n.s.			
lGPi	n.s.				n.s.			
lVL	n.s.				n.s.			
lVPL	n.s.				n.s.			
lSMA	n.s.				3.19	−4	4	44
lSMC	n.s.				n.s.			
lPMv	n.s.				n.s.			
rCB	n.s.				n.s.			
rDN	n.s.				n.s.			
ET movement								
rPut	n.s.				n.s.			
rGPi	n.s.				n.s.			
rVL	n.s.				n.s.			
rVPL	n.s.				n.s.			
rSMA	n.s.				n.s.			
rSMC	n.s.				n.s.			
rPMv	n.s.				n.s.			
lCB	3.84	−26	−50	−20	n.s.			
lDN	n.s.				n.s.			
lPut	n.s.				n.s.			
lGPi	n.s.				n.s.			
lVL	n.s.				n.s.			
lVPL	n.s.				n.s.			
lSMA	n.s.				n.s.			
lSMC	n.s.				n.s.			
lPMv	n.s.				n.s.			
rCB	n.s.				n.s.			
rDN	n.s.				n.s.			

Z-values refer to activation maxima within the respective region, $p<0.001$ uncorrected, height threshold $Z>3.09$.

0.69±0.16 Hz (mean±SD), slow movements were performed at 1.00±0.25 Hz, moderate movements were performed at 1.84± 0.58 Hz, fast movements were performed at 2.95±0.78 Hz, and very fast movements were performed at 4.03±0.94 Hz during SI movements; as in the present study, ET movement rates were almost identical to the rates of the auditory triggers (0.5 Hz trigger, 0.51±0.02 Hz; 1 Hz trigger, 1.00±0.01 Hz; 2 Hz trigger, 1.99± 0.02 Hz; 3 Hz trigger, 3.01±0.07 Hz; 4 Hz trigger, 3.97± 0.07 Hz). No statistical difference was observed between young and aged subjects ($p=0.626$ in SI movements and $p=0.131$ in ET movements, determined by two-way ANOVA with repeated measures), although there was a tendency toward slower movement during the SI task and increased variability in frequency during ET task in aged subjects compared with young subjects.

Foci of activation

Within group analysis in aged subjects

To separate regional activities within the same task but with different rate–response functions, a parametric approach based on orthogonal basic functions up to the fourth order was used. In the study of main effects, both tasks caused significant activation in the bilateral posterior Put, VL, VPL, SMA, SMC, PMv, DN, CB and the right GP (Table 1; Figs. 2A and B) in the aged subjects, consistent with the results in young subjects previously reported (Taniwaki et al., 2006).

A significant positive linear increase in the magnitude of the BOLD response in parallel with rate of finger movement was seen in the right SMC, PMv and DN, and the left VPL, SMC and PMv during SI tasks (Table 1; Fig. 2C). There was a tendency toward a linear increase in the activation of the left CB. In ET tasks, a significant positive linear increase was detected in the right SMA, left SMC, bilateral CB and DN, and a tendency toward a linear increase in activation was observed in the right SMC and PMv (Table 1; Fig. 2D).

Neither a significant non-linear rate–response function (2nd order), nor a negative linear correlation in terms of a decline in BOLD response in parallel with tapping rate, was documented in BGTM or CC loops.

Between-group analysis of brain activity

Compared with young subjects, aged subjects had greater activation in the left SMC during SI tasks and in the left SMA and SMC during ET tasks in a study of main effects (Table 2; Fig. 3). There was greater activation in the right SMC during SI tasks and in the left CB during ET tasks in young subjects compared with aged subjects in the main effects analysis (Table 3; Fig. 4). In the analysis of linear effects, young subjects showed greater

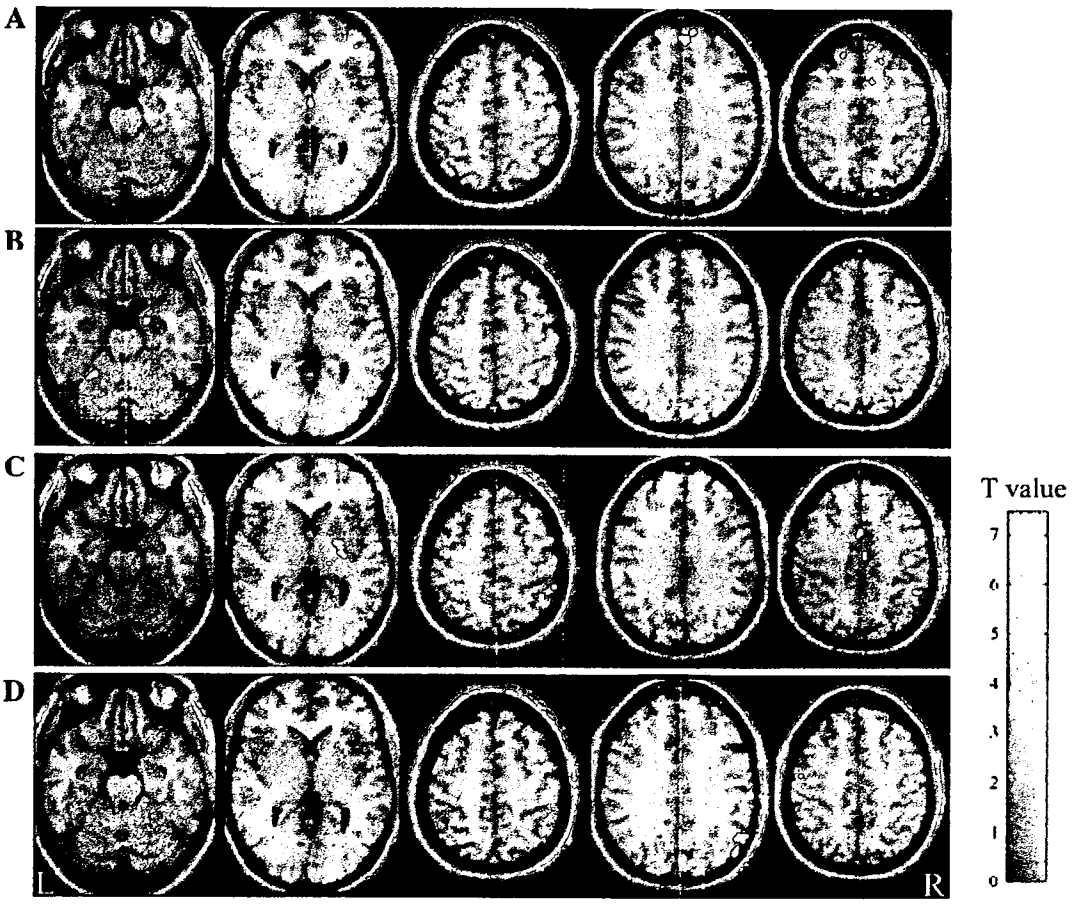

Fig. 4. Brain areas with more activation in young subjects than in aged subjects. Regions showing main effects of movement rate (A and B) and a significant linear relationship between BOLD signal and increasing movement rate (C and D). All regions are significant at the level of $p<0.001$, uncorrected.

activation in the right Put, VL, VPL, SMA and left SMA during SI movement.

Structural equation modeling

The results of mapping experiments on aged subjects suggest that the bilateral motor cortices contribute more to the rate-dependent motor processing than the subcortical motor loops. To confirm this hypothesis, functional network analysis was performed.

Within-group analysis of structural equation modeling in aged subjects

The omnibus test showed that the functional networks in the right hemisphere and left cerebellum differed significantly between the two tasks in aged subjects [χ^2 diff(29)=387.37, $p<0.001$]. Functional interactions from the right SMC to the right VL, and those from the right PMv to the right SMC were stronger during SI tasks. There were moderate interactions from the right SMA to the right SMC during both tasks (Table 5; Figs. 5C and D).

Functional networks in the left hemisphere and right cerebellum differed significantly between the two tasks according to the omnibus test [χ^2 diff(29)=327.54, $p<0.001$]. Interactions from the left GPi to the left VL were stronger during SI tasks, whereas those from the left PMv to the left SMA were stronger during ET tasks.

Interhemisphere SEM in SI tasks resulted in a model that was different from that generated during the ET task [χ^2 diff(12)= 271.01, $p<0.001$]. Interactions from the left to right PMv were stronger during SI movements; by contrast, the interactions from the right SMA to the left SMC, those from the left to right SMC, and those from the left SMA to right PMv were stronger during ET tasks. Moderate interactions between both SMAs were observed in both tasks.

Between-group analysis of structural equation modeling

The functional networks in the right hemisphere and left cerebellum differed significantly between the two groups of subjects according to the omnibus test of data collected during SI tasks [χ^2 diff(29)=1078.72, $p<0.001$] and ET tasks [χ^2 diff(29)= 280.71, $p<0.001$]. During SI tasks, BGTM interactions from the right SMA to the right SMC, via the right Put, right GPi and right VL, were stronger in young subjects than in aged subjects, whereas the interactions from the right SMA to the right SMC

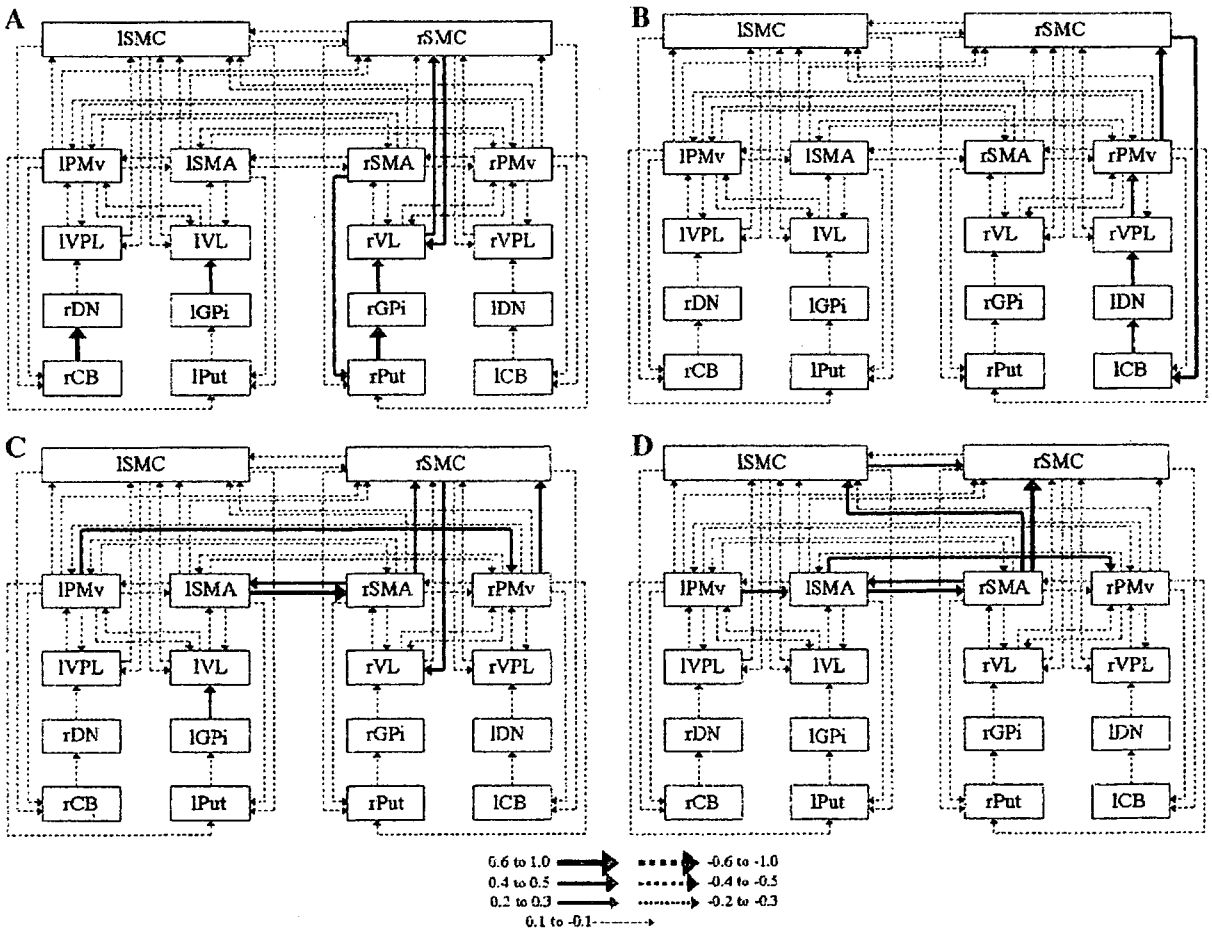

Fig. 5. Schematic representation of the results of structural equation modeling in young (A and B) and aged subjects (C and D). (A and C) Self-initiated movements. (B and D) Externally triggered movements. Positive coefficients (solid arrows) indicate interactions in which an increase in activity in one area is associated with an increase in activity in the other area. Negative coefficients (broken arrows) indicate opposite interactions.

Table 4
Interregional correlation coefficients (Pearson product-moment correlation (A) and path coefficients (B) during two different tasks in young subjects

	rPut	rGP	rVL	rVPL	rSMA	rSMC	rPMv	lDN	lCB	lPut	lGP	lVL	lVPL	lSMA	lSMC	lPMv	rDN	rCB
A																		
	SI																	
rPut	1.00																	
rGP	0.53	1.00																
rVL	0.05	0.26	1.00															
rVPL	0.19	0.20	0.17	1.00														
rSMA	0.24	0.06	0.11	0.00	1.00													
rSMC	0.00	0.04	0.33	0.06	−0.03	1.00												
rPMv	0.10	−0.02	0.17	0.03	−0.01	0.21	1.00											
lDN	0.25	0.16	0.00	0.17	0.04	0.00	−0.03	1.00										
lCB	0.21	0.08	0.08	0.10	0.06	0.17	0.01	0.18	1.00									
lPut	0.20	0.25	−0.01	0.22	−0.02	−0.12	0.07	0.16	0.02	1.00								
lGP	0.14	0.16	0.14	0.17	−0.07	0.13	0.11	0.21	0.06	0.17	1.00							
lVL	0.11	0.13	0.46	0.18	0.16	0.17	0.09	0.05	0.07	0.06	0.21	1.00						
lVPL	0.11	0.16	0.28	0.33	0.09	0.01	0.03	0.15	0.02	0.16	0.16	0.42	1.00					
lSMA	0.12	0.11	0.03	−0.01	0.18	−0.06	0.03	0.07	−0.05	0.08	0.00	0.14	0.04	1.00				
lSMC	0.05	0.06	0.05	0.03	0.17	0.20	0.01	0.12	0.07	−0.03	0.04	0.16	0.06	0.02	1.00			
lPMv	0.07	0.07	−0.02	0.12	0.15	0.03	−0.02	0.14	−0.02	0.07	0.09	−0.03	0.03	0.14	0.16	1.00		
rDN	0.26	0.21	0.06	0.16	0.08	0.02	−0.02	0.43	0.21	0.10	0.21	0.16	0.06	0.03	0.07	0.02	1.00	
rCB	0.08	0.00	−0.09	−0.08	0.06	0.01	−0.03	0.05	0.29	0.06	−0.02	0.02	−0.04	0.06	0.09	0.00	0.41	1.00
	ET																	
rPut	1.00																	
rGP	0.17	1.00																
rVL	−0.01	0.16	1.00															
rVPL	0.01	0.18	0.35	1.00														
rSMA	−0.02	0.14	0.17	0.08	1.00													
rSMC	0.11	0.10	0.12	0.10	0.13	1.00												
rPMv	0.17	0.06	0.04	0.23	0.04	0.22	1.00											
lDN	0.23	0.15	0.12	0.22	0.06	0.12	0.00	1.00										
lCB	0.02	−0.06	0.16	0.04	0.09	0.28	0.08	0.26	1.00									
lPut	0.16	0.09	0.07	0.11	0.11	0.11	0.11	0.14	0.00	1.00								
lGP	0.10	0.19	0.20	0.18	0.14	0.06	0.04	0.11	0.05	0.13	1.00							
lVL	−0.10	0.23	0.25	0.21	0.15	0.03	0.16	0.03	0.00	0.08	0.15	1.00						
lVPL	0.19	0.33	0.28	0.26	0.07	−0.01	0.17	0.19	0.02	0.14	0.26	0.50	1.00					
lSMA	0.10	0.14	0.12	0.03	0.17	0.10	0.09	0.03	−0.03	0.02	0.12	0.14	0.15	1.00				
lSMC	0.29	0.06	−0.12	−0.05	0.08	0.15	0.17	0.16	0.14	−0.04	−0.03	0.02	0.10	0.10	1.00			
lPMv	0.08	0.02	0.01	−0.06	0.06	0.06	0.11	−0.06	0.08	0.08	0.03	0.01	0.04	0.11	0.05	1.00		
rDN	0.16	−0.12	−0.13	0.00	0.00	0.08	−0.03	0.33	0.18	0.11	0.10	0.07	0.12	0.02	0.15	0.05	1.00	
rCB	0.05	−0.09	−0.04	0.00	−0.06	−0.04	0.00	0.10	0.22	−0.09	−0.02	0.03	−0.04	−0.06	0.08	−0.02	0.18	1.00
B																		
	SI																	
rPut	–	–	–	–	0.24	−0.03	0.10	–	–	–	–	–	–	–	–	–	–	–
rGP	0.53	–	–	–	–	–	–	–	–	–	–	–	–	–	–	–	–	–
rVL	–	0.24	–	–	0.08	0.22	0.09	–	–	–	–	–	–	–	–	–	–	–
rVPL	–	–	–	–	–	0.06	0.03	0.17	–	–	–	–	–	–	–	–	–	–
rSMA	–	–	0.08	–	–	–	−0.02	–	–	–	–	–	–	0.12	–	0.10	–	–
rSMC	–	–	0.24	−0.01	−0.06	–	0.16	–	–	–	–	–	–	−0.07	0.15	0.02	–	–
rPMv	–	–	0.13	0.00	−0.02	–	–	–	–	–	–	–	–	0.03	–	−0.02	–	–
lDN	–	–	–	–	–	–	–	–	0.18	–	–	–	–	–	–	–	–	–
lCB	–	–	–	–	–	0.18	−0.03	–	–	–	–	–	–	–	–	–	–	–
lPut	–	–	–	–	–	–	–	–	–	–	–	–	–	0.07	−0.04	0.07	–	–
lGP	–	–	–	–	–	–	–	–	–	0.17	–	–	–	–	–	–	–	–
lVL	–	–	–	–	–	–	–	–	–	–	0.21	–	–	0.12	0.12	−0.07	–	–
lVPL	–	–	–	–	–	–	–	–	–	–	–	–	–	–	0.09	−0.05	0.06	–
lSMA	–	–	–	–	0.14	–	0.02	–	–	–	–	0.11	–	–	–	0.11	–	–
lSMC	–	–	–	–	0.17	0.16	−0.02	–	–	–	–	0.15	−0.03	−0.03	–	0.17	–	–
lPMv	–	–	–	–	0.12	–	−0.01	–	–	–	–	−0.06	0.06	0.11	–	–	–	–
rDN	–	–	–	–	–	–	–	–	–	–	–	–	–	–	–	–	–	0.41
rCB	–	–	–	–	–	–	–	–	–	–	–	–	–		0.09	−0.02	–	–

(continued on next page)

Table 4 (*continued*)

	rPut	rGP	rVL	rVPL	rSMA	rSMC	rPMv	lDN	lCB	lPut	lGP	lVL	lVPL	lSMA	lSMC	lPMv	rDN	rCB
B																		
	ET																	
rPut	–	–	–	–	−0.04	0.08	0.15	–	–	–	–	–	–	–	–	–	–	–
rGP	0.17	–	–	–	–	–	–	–	–	–	–	–	–	–	–	–	–	–
rVL	–	0.14	–	–	0.10	0.06	0.03	–	–	–	–	–	–	–	–	–	–	–
rVPL	–	–	–	–	–	0.02	−0.02	0.21	–	–	–	–	–	–	–	–	–	–
rSMA	–	–	0.14	–	–	–	0.03	–	–	–	–	–	–	0.13	–	0.03	–	–
rSMC	–	–	0.07	0.01	0.11	–	0.21	–	–	–	–	–	–	0.08	0.12	0.05	–	–
rPMv	–	–	−0.07	0.26	0.02	–	–	–	–	–	–	–	–	0.06	–	0.08	–	–
lDN	–	–	–	–	–	–	–	–	0.26	–	–	–	–	–	–	–	–	–
lCB	–	–	–	–	–	0.28	0.02	–	–	–	–	–	–	–	–	–	–	–
lPut	–	–	–	–	–	–	–	–	–	–	–	–	–	0.02	−0.05	0.08	–	–
lGP	–	–	–	–	–	–	–	–	–	0.13	–	–	–	–	–	–	–	–
lVL	–	–	–	–	–	–	–	–	–	–	0.14	–	–	0.09	0.03	0.00	–	–
lVPL	–	–	–	–	–	–	–	–	–	–	–	–	–	–	−0.06	−0.01	0.13	–
lSMA	–	–	–	–	0.13	–	0.07	–	–	–	–	0.11	–	–	–	0.08	–	–
lSMC	–	–	–	–	−0.07	0.07	0.15	–	–	–	–	−0.07	0.14	0.08	–	0.04	–	–
lPMv	–	–	–	–	−0.05	–	0.08	–	–	–	–	−0.03	0.04	0.08	–	–	–	–
rDN	–	–	–	–	–	–	–	–	–	–	–	–	–	–	–	–	–	0.18
rCB	–	–	–	–	–	–	–	–	–	–	–	–	–	–	0.08	−0.02	–	–

and those from the right PMv to right SMC were stronger in aged subjects. There were moderate interactions from the right SMC to the right VL in both subjects. During ET tasks, entire CC interactions from the left CB to the left CB, via the left DN, right VPL, right PMv and right SMC, were stronger in young subjects. By contrast, interaction from the right SMA to the right SMC was stronger in aged subjects (Tables 4, 5; Fig. 5).

The omnibus test suggested that the functional networks of the left hemisphere and right cerebellum are different between the young and aged groups during both SI [χ^2 diff(29)=344.92, $p<0.001$] and ET tasks [χ^2 diff(29)=255.01, $p<0.001$]. During SI tasks, moderate interactions were seen from the left GPi to the left VL in both groups. In addition, the interactions from the right CB to the right DN were stronger in the young group than in the aged group. During ET tasks, the interactions from the left PMv to the left SMA were stronger in the aged group.

The results of interhemisphere SEM were different between young and aged groups during both SI [χ^2 diff(12)=2013.49, $p<0.001$] and ET tasks [χ^2 diff(12)=2404.69, $p<0.001$]. Only the old group showed moderate interactions between hemispheres. During SI tasks, there were stronger interactions from the left PMv to right PMv in the aged group. During ET tasks, interhemispheric interactions from the left SMA to right PMv, those from the left SMC to the right SMC and those from the right SMA to the left SMC were stronger in the aged group. There were stronger reciprocal influences among bilateral SMAs in the aged group during both tasks.

Discussion

In the current study, we compared functional interactions within the BGTM and CC loops between young and aged subjects using fMRI combined with a parametric approach and SEM, during sequential finger movements of SI and ET tasks. The major new findings in aged subjects were as follows: (1) decreased connectivity within BGTM loops during SI movements, (2) decreased connectivity within CC loops during ET movements and (3) increased connectivity within motor cortices and between hemispheres during both types of movement.

Decreased connectivity within BGTM loop during SI task

Normal aging is characterized by impaired motor ability (Calautti et al., 2001; Mattay et al., 2002; Sailer et al., 2000; Welford, 1988). In particular, slowing of motor movements and loss of fine motor skills are thought to reflect underlying age-related degeneration in brain systems subserving motor function (Smith et al., 1999). The basal ganglia are subcortical nuclei that are thought to be motor structures involved in the timing of movements (O'Boyle et al., 1996; Pastor et al., 1992, 2004), the speed of movement and the acquisition of motor skills (Laforce and Doyon, 2002; Vakil et al., 2000). Concerning the contribution of lower sensorimotor processes to behavioral slowing in the elderly, Kaasinen et al. (2000) have documented the decline of the dopaminergic neurotransmitter system in the aging human brain and, more specifically, the loss of dopamine receptors in the striatum and extrastriatal regions, which is associated with a basic impairment in motor functions (Volkow et al., 1998). These results suggest decreased activity in the regions within the BGTM loop in aged subjects.

Although several functional brain imaging studies have reported age-related changes in human motor system, only a few studies have reported age-related changes in the striatum. In an fMRI study of a visually paced button press task using the right hand, aged subjects showed additional areas of activation in the bilateral Put (Mattay et al., 2002). Aged subjects showed greater *activation* in the ipsilateral Put and less activation in the contralateral Put, when either making a fist or opposing the thumb and index finger with left hand (Fang et al., 2005). Studies of self-initiated, memorized sequential right finger movements (Wu and Hallett, 2005), visually paced isometric hand grip tasks using each hand (Ward and Frackowiak, 2003), auditory paced finger and wrist movements of each hand (Hutchinson et al., 2002) and auditory paced thumb to index tapping with either hand (Calautti et al., 2001) failed to show any age-related change in the activation of the striatum. Thus, the results of previous functional brain imaging studies were inconsistent. Basically, these studies performed categorical comparisons of fMRI and PET data and could only show the change in activation in each

Table 5
Interregional correlation coefficients (Pearson product-moment correlation (A) and path coefficients (B) during two different tasks in aged subjects

	rPut	rGP	rVL	rVPL	rSMA	rSMC	rPMv	lDN	lCB	lPut	lGP	lVL	lVPL	lSMA	lSMC	lPMv	rDN	rCB
A																		
	SI																	
rPut	1.00																	
rGP	0.19	1.00																
rVL	0.18	0.16	1.00															
rVPL	0.27	0.20	0.29	1.00														
rSMA	0.05	0.02	0.02	0.02	1.00													
rSMC	0.17	0.08	0.26	0.21	0.30	1.00												
rPMv	0.10	0.13	0.19	0.11	0.12	0.29	1.00											
lDN	0.08	0.05	0.19	0.18	0.10	0.21	0.14	1.00										
lCB	0.00	0.03	0.15	0.04	−0.02	0.05	−0.04	0.15	1.00									
lPut	0.25	0.22	0.13	0.18	−0.05	0.03	0.18	0.13	0.10	1.00								
lGP	0.21	0.30	0.27	0.19	0.09	0.06	0.15	0.05	0.10	0.17	1.00							
lVL	0.13	0.24	0.54	0.27	0.00	0.10	0.11	0.15	0.16	0.18	0.30	1.00						
lVPL	0.25	0.22	0.38	0.28	0.01	0.12	0.15	0.15	0.19	0.26	0.27	0.52	1.00					
lSMA	0.09	0.09	−0.01	0.04	0.55	0.21	0.14	0.07	−0.07	0.02	0.06	−0.02	0.01	1.00				
lSMC	0.06	0.06	0.04	0.07	0.03	0.09	0.19	0.09	−0.02	0.12	0.06	0.04	0.13	0.12	1.00			
lPMv	0.16	0.21	0.18	0.16	0.09	0.19	0.28	0.14	0.00	0.08	0.11	0.15	0.08	0.20	0.17	1.00		
rDN	0.08	0.05	0.15	0.11	0.09	0.20	0.20	0.37	0.21	0.05	0.04	0.13	0.10	0.04	0.05	0.10	1.00	
rCB	−0.01	0.04	0.05	0.01	−0.05	−0.01	−0.04	0.11	0.49	0.12	−0.01	0.12	0.22	−0.04	0.02	−0.04	0.13	1.00
	ET																	
rPut	1.00																	
rGP	0.06	1.00																
rVL	0.13	0.00	1.00															
rVPL	0.15	0.16	0.20	1.00														
rSMA	0.08	0.00	0.06	0.08	1.00													
rSMC	0.03	0.00	0.04	0.08	0.46	1.00												
rPMv	0.05	0.09	0.03	0.10	0.24	0.20	1.00											
lDN	0.12	0.08	0.17	0.13	0.07	0.15	0.09	1.00										
lCB	0.04	0.03	0.10	0.01	0.12	−0.02	−0.05	0.10	1.00									
lPut	0.09	0.20	0.13	0.26	0.06	0.02	0.03	0.11	0.09	1.00								
lGP	0.16	0.21	0.09	0.17	0.01	0.05	0.01	0.08	0.07	0.10	1.00							
lVL	0.12	0.11	0.53	0.19	0.13	0.09	0.07	0.17	0.09	0.16	0.05	1.00						
lVPL	0.15	0.02	0.28	0.21	0.04	0.01	0.05	0.14	0.01	0.20	0.08	0.33	1.00					
lSMA	0.16	0.01	0.07	0.00	0.49	0.20	0.28	0.08	0.04	0.03	−0.02	0.08	0.13	1.00				
lSMC	0.07	−0.05	0.18	0.09	0.36	0.34	0.07	0.10	0.18	0.10	0.08	0.11	0.09	0.18	1.00			
lPMv	0.11	0.08	0.11	0.09	0.15	0.03	0.15	0.05	−0.03	0.08	0.03	0.08	0.17	0.26	0.11	1.00		
rDN	0.12	0.04	0.10	0.20	−0.07	0.00	0.03	0.28	0.12	0.11	−0.07	0.14	0.12	−0.01	0.03	−0.01	1.00	
rCB	0.02	0.03	0.10	−0.01	−0.12	−0.13	0.00	0.03	0.33	0.05	0.01	0.05	−0.04	0.01	−0.02	0.04	0.06	1.00
B																		
	SI																	
rPut	–	–	–	–	0.00	0.15	0.05	–	–	–	–	–	–	–	–	–	–	–
rGP	0.19	–	–	–	–	–	–	–	–	–	–	–	–	–	–	–	–	–
rVL	–	0.13	–	–	−0.06	0.20	0.08	–	–	–	–	–	–	–	–	–	–	–
rVPL	–	–	–	–	–	0.01	0.01	0.18	–	–	–	–	–	–	–	–	–	–
rSMA	–	–	0.00	–	–	–	0.09	–	–	–	–	–	–	0.41	–	−0.02	–	–
rSMC	–	–	0.11	0.15	0.27	–	0.21	–	–	–	–	–	–	0.18	0.04	0.15	–	–
rPMv	–	–	0.13	0.07	0.09	–	–	–	–	–	–	–	–	0.08	–	0.20	–	–
lDN	–	–	–	–	–	–	–	–	0.15	–	–	–	–	–	–	–	–	–
lCB	–	–	–	–	–	0.07	−0.06	–	–	–	–	–	–	–	–	–	–	–
lPut	–	–	–	–	–	–	–	–	–	–	–	–	–	−0.01	0.11	0.06	–	–
lGP	–	–	–	–	–	–	–	–	–	0.17	–	–	–	–	–	–	–	–
lVL	–	–	–	–	–	–	–	–	–	–	0.29	–	–	−0.05	0.04	0.08	–	–
lVPL	–	–	–	–	–	–	–	–	–	–	–	–	–	–	−0.07	0.10	0.09	–
lSMA	–	–	–	–	0.39	–	0.06	–	–	–	–	−0.03	–	–	–	0.16	–	–
lSMC	–	–	–	–	0.00	0.03	0.18	–	–	–	–	−0.09	0.18	0.09	–	0.15	–	–
lPMv	–	–	–	–	0.07	–	0.21	–	–	–	–	0.14	−0.02	0.15	–	–	–	–
rDN	–	–	–	–	–	–	–	–	–	–	–	–	–	–	–	–	–	0.13
rCB	–	–	–	–	–	–	–	–	–	–	–	–	–	–	0.03	−0.04	–	–

(continued on next page)

Table 5 (*continued*)

	rPut	rGP	rVL	rVPL	rSMA	rSMC	rPMv	lDN	lCB	lPut	lGP	lVL	lVPL	lSMA	lSMC	lPMv	rDN	rCB
B																		
	ET																	
rPut	–	–	–	–	0.08	−0.01	0.03	–	–	–	–	–	–	–	–	–	–	–
rGP	0.06	–	–	–	–	–	–	–	–	–	–	–	–	–	–	–	–	–
rVL	–	0.00	–	–	0.04	0.01	0.02	–	–	–	–	–	–	–	–	–	–	–
rVPL	–	–	–	–	–	0.02	0.00	0.13	–	–	–	–	–	–	–	–	–	–
rSMA	–	–	0.04	–	–	–	0.18	–	–	–	–	–	–	0.37	–	0.01	–	–
rSMC	–	–	0.00	0.03	0.44	–	0.09	–	–	–	–	–	–	0.16	0.28	−0.04	–	–
rPMv	–	–	−0.01	0.09	0.18	–	–	–	–	–	–	–	–	0.22	–	0.06	–	–
lDN	–	–	–	–	–	–	–	–	0.10	–	–	–	–	–	–	–	–	–
lCB	–	–	–	–	–	−0.01	−0.05	–	–	–	–	–	–	–	–	–	–	–
lPut	–	–	–	–	–	–	–	–	–	–	–	–	–	−0.01	0.09	0.07	–	–
lGP	–	–	–	–	–	–	–	–	–	0.10	–	–	–	–	–	–	–	–
lVL	–	–	–	–	–	–	–	–	–	–	0.04	–	–	0.04	0.07	0.06	–	–
lVPL	–	–	–	–	–	–	–	–	–	–	–	–	–	–	0.05	0.03	0.12	–
lSMA	–	–	–	–	0.33	–	0.12	–	–	–	–	0.04	–	–	–	0.20	–	–
lSMC	–	–	–	–	0.31	0.11	−0.03	–	–	–	–	0.06	0.03	0.16	–	0.06	–	–
lPMv	–	–	–	–	0.12	–	0.10	–	–	–	–	0.00	0.14	0.18	–	–	–	–
rDN	–	–	–	–	–	–	–	–	–	–	–	–	–	–	–	–	–	0.06
rCB	–	–	–	–	–	–	–	–	–	–	–	–	–	–	−0.02	0.04	–	–

region. Instead, we used correlation data based on rate-dependent movements and SEM. SEM has provided new insights into task-specific functional networks (Grafton et al., 1994; McIntosh and Gonzalez-Lima, 1994; McIntosh et al., 1994). Our approach provides additional information about brain physiology such as rhythm formation, motor preparation and motor execution that is not always apparent in the results of categorical comparisons of fMRI data (Taniwaki et al., 2006). Consistent with clinical (Smith et al., 1999) and pathological studies (Kaasinen et al., 2000; Volkow et al., 1998), our current mapping study shows less activation in the right Put, VL and bilateral SMA in the aged group compared with the young group during SI movements. Our SEM results further indicate an age-dependent decline in connectivity within BGTM loops during SI tasks. To our knowledge, we are the first to show an age-related decrease in connectivity within the BGTM loop. Our aged group also showed the tendency toward slower movement during the SI task. Because the BGTM loop is suggested to play an important role in central timing processes (in the SMA, basal ganglia and VL) and execution processes in the SMC (Taniwaki et al., 2003; 2006), age-related decline of either central timing processes and/or execution processes might reflect the decreased connectivity within BGTM loop and slower movement during the SI task.

Decreased connectivity within the CC loop during ET tasks

The cerebellum also plays an important role as a motor structure (Casini and Ivry, 1999; Ivry et al., 1988; Laforce and Doyon, 2002) and is involved in the execution of fine motor skills which are lost during aging (Smith et al., 1999). *Anatomically*, significant changes are observed with age in the anterior lobe, where a selective 40% loss of both Purkinje and granule cells was observed in the cerebellum. Furthermore, a 30% loss of volume, mostly due to loss of cortical volume, was observed in the anterior lobe, which is predominantly involved in motor control (Andersen et al., 2003). Thus, decreased activity within the CC loop can be predicted.

Several functional brain imaging studies have reported age-related changes in the cerebellum. fMRI studies of a visually paced button press task using right hand (Mattay et al., 2002) and self-initiated, memorized sequential right finger movements (Wu and Hallett, 2005) demonstrated greater activation in the bilateral cerebellar cortex in aged subjects compared with young subjects. In an fMRI study of a visually paced isometric hand grip task using each hand, aged subjects showed additional areas of activation in the cerebellar vermis (Ward and Frackowiak, 2003). By contrast, aged subjects showed less activation in bilateral cerebellum by auditory paced right finger or wrist movement and in the left cerebellum during left wrist movement compared with young subjects in an fMRI study (Hutchinson et al., 2002). A PET study also showed no age-related change in the cerebellum during auditory paced thumb to index tapping with either hand (Calautti et al., 2001). Previous imaging studies of regional activation in the cerebellum have failed to show consistent results, though the tasks were different from each other.

Consistent with clinical study (Smith et al., 1999) and anatomical study (Andersen et al., 2003), our SEM results indicate an age-dependent decline in connectivity within CC loops during ET tasks. Our aged group also showed the tendency toward increased variability in frequency in the ET task. Because the CC loop is involved in the functions of the cerebellum in monitoring and adjusting inputs from SMC, as well as motor planning processes in the PMv and execution processes in the SMC (Taniwaki et al., 2003; 2006), age-related alteration in these functions might bring about not only decreased connectivity within the CC loop, but also the tendency toward increased variability in frequency.

Increased connectivity within motor cortices

Our SEM showed increased connectivity within motor cortices and between cerebral hemispheres. In SI tasks, moderate interactions were observed from the right SMA to the right SMC, from the right PMv to the right SMC, and the left PMv to right PMv in the aged subjects. Bilateral SMAs showed moderate positive reciprocal influences. The role of the SMA in behavior remains elusive, but many functions have been ascribed to this region including internal planning (Tanji and Shima, 1994), timing (Macar et al., 2004), sequencing (Shima and Tanji, 1998) and action retrieval (Chen et al., 1995). Our results from the ET tasks

showed that aged subjects have stronger interactions among the bilateral PMv, SMA and SMC, which reflect motor planning processes in the PMv and execution processes in the SMC. Since this connectivity in the aged group includes neither the basal ganglia nor the cerebellum, intercortical interactions might be strengthened for good motor performance.

Interhemispheric interactions were more obvious in aged subjects than in young subjects. It is possible that these interhemispheric interactions represent either transcallosal inhibition or facilitation. SEM results need to be interpreted carefully because of methodological limitations. We cannot always interpret a positive path coefficient as an excitatory influence and a negative path coefficient as inhibitory (McIntosh and Gonzalez-Lima, 1994). Instead, positive and negative path coefficients measure signs of covariance relationships among the structures of a network. Our finding of stronger interhemispheric interactions in aged subjects could be regarded as reflecting quantitative changes within a functional network that may be comparable to reduced functional lateralization in the aged motor cortex (Naccarato et al., 2006). These differences might be more related to the greater demands in aged subjects on maintaining and updating working memory, attending to multiple actions and/or response conflict monitoring.

Previous imaging studies have shown greater activation of motor cortices in elderly subjects, in both spatial extent and magnitude (Esposito et al., 1999; Grady, 2000; Hutchinson et al., 2002; Mattay et al., 2002; Wu and Hallett, 2005). A recent study using rTMS and PET reported enhanced local effective connectivity between motor-related areas in aged subjects (Rowe et al., 2006). Our current results also showed increased connectivity within motor cortices and between hemispheres. Several imaging studies of motor behavior provide support for the interpretation that greater activity is a compensatory response to increased functional demands (Hutchinson et al., 2002; Mattay et al., 2002; Wu and Hallett, 2005), although a recent study did not support this interpretation (Riecker et al., 2006). The increased interactions within motor cortices in our elderly subjects may also be a consequence of the reorganization and redistribution that takes place in brain circuitry in response to neurodegeneration (Mattay et al., 2002; Wu and Hallett, 2005). It is possible that increased connectivity within motor cortices is the product of a breakdown in local inhibitory processes, secondary to neural degeneration leading to intracortical disconnectivity (Mattay et al., 2002).

Concluding remarks

A combined use of sequential finger movements, fMRI and SEM enabled us to visualize the effects of age on functional connectivity within motor loops in the basal ganglia and cerebellum during motor execution. Different functional interactions within cortico-subcortical loops and intracortical loops were demonstrated. The functional changes that occur in the BGTM and CC loops in neurological disorders remain to be determined; analysis of patients with Parkinson's disease, currently progress in our laboratory, will help to address this question.

References

Alexander, G.E., Crutcher, M.D., Delong, M.R., 1990. Basal ganglia thalamo-cortical circuits: parallel substrates for motor, oculomotor, "prefrontal" and "limbic" functions. Prog. Brain Res. 85, 119–146.

Andersen, B.B., Gundersen, H.J.G., Pakkenberg, B., 2003. Aging of the human cerebellum: a stereological study. J. Comp. Neurol. 466, 356–365.

Barbas, H., Pandya, D.N., 1987. Architecture and frontal cortical connections of the premotor cortex (area 6) in the rhesus monkey. J. Comp. Neurol. 256, 211–228.

Bullmore, E., Horwitz, B., Honey, G., Brammer, M., Williams, S., Sharma, T., 2000. How good is good enough in path analysis of fMRI data? NeuroImage 11, 289–301.

Büchel, C., Wise, R.J.S., Mummery, C.J., Poline, J.-B., Friston, K.J., 1996. Nonlinear regression in parametric activation studies. NeuroImage 4, 60–66.

Büchel, C., Holmes, A.P., Rees, G., Friston, K.J., 1998. Characterizing stimulus–response functions using nonlinear regressors in parametric fMRI experiments. NeuroImage 8, 140–148.

Calautti, C., Serrati, C., Baron, J.C., 2001. Effects of age on brain activation during auditory-cued thumb-to-index opposition: a positron emission tomography study. Stroke 32, 139–146.

Casini, L., Ivry, R.B., 1999. Effects of divided attention on temporal processing in patients with lesions of the cerebellum or frontal lobe. Neuropsychology 13, 10–21.

Chen, Y.-C., Thaler, D., Nixon, P.D., Stern, C.E., Passingham, R.E., 1995. The functions of the medial premotor cortex (SMA) II. The timing and selection of learned movements. Exp. Brain Res. 102, 461–473.

Delong, M.R., 1990. Primate models of movement disorders of basal ganglia origin. Trends Neurosci. 13, 281–285.

Esposito, G., Kirkby, B.S., Van Horn, J.D., Ellmore, T.M., Berman, K.F., 1999. Context-dependent, neural system-specific neurophysiological concomitants of ageing: mapping PET correlates during cognitive activation. Brain 122, 963–979.

Fang, M., Li, J., Lu, G., Gang, X., Yew, D.T., 2005. A fMRI study of age-related differential cortical patterns during cued motor movement. Brain Topogr. 17, 127–137.

Friston, K.J., Holmes, A.P., Worsley, K.J., Poline, J.-P., Frith, C.D., Frackowiak, R.S., 1995. Statistical parametric maps in functional imaging: a general linear approach. Hum. Brain Mapp. 2, 189–210.

Friston, K.J., Holmes, A.P., Worsley, K.J., 1999. How many subjects constitute a study? NeuroImage 10, 1–5.

Grady, C.L., 2000. Functional brain imaging and age-related changes in cognition. Biol. Psychol. 54, 259–281.

Grafton, S.T., Sutton, J., Couldwell, W., Lew, M., Waters, C., 1994. Network analysis of motor system connectivity in Parkinson's disease: modulation of thalamocortical interactions after pallidotomy. Hum. Brain Mapp. 2, 45–55.

Hedden, T., Gabrieli, J.D., 2004. Insights into the ageing mind: a view from cognitive neuroscience. Nat. Rev., Neurosci. 5, 87–96.

Hutchinson, S., Kobayashi, M., Horkan, C.M., Pascual-Leone, A., Alexander, M.P., Schlaug, G., 2002. Age-related differences in movement representation. NeuroImage 17, 1720–1728.

Ivry, R.B., Keele, S.W., Diener, H.C., 1988. Dissociation of the lateral and medial cerebellum in movement timing and movement execution. Exp. Brain Res. 73, 167–180.

Jancke, L., Specht, K., Mirzazade, S., Peters, M., 1999. The effect of finger-movement speed of the dominant and subdominant hand on cerebellar activation: a functional magnetic resonance imaging study. NeuroImage 9, 497–507.

Johnson, P.B., Ferraina, S., Bianchi, L., Caminiti, R., 1996. Cortical networks for visual reaching: physiological and anatomical organization of frontal and parietal lobe arm regions. Cereb. Cortex 6, 102–119.

Kaasinen, V., Vilkman, H., Hietala, J., Nagren, K., Helenius, H., Olsson, H., Farde, J., 2000. Age-related dopamine D2/D3 receptor loss in extrastriatal regions of the human brain. Neurobiol. Aging 21, 683–688.

Kelly, R.M., Strick, P.L., 2003. Cerebellar loops with motor cortex and prefrontal cortex of a nonhuman primate. J. Neurosci. 23, 8432–8444.

Kondo, H., Morishita, M., Osaka, N., Osaka, M., Fukuyama, H., Shibasaki, H., 2004. Functional roles of the cingulo-frontal network in performance on working memory. NeuroImage 21, 2–14.

Laforce, R., Doyon, J., 2002. Differential role for the striatum and cerebellum in response to novel movements using motor learning paradigm. Neuropsychologia 40, 512–517.

Macar, F., Anton, J.L., Bonnet, M., Vidal, F., 2004. Timing functions of the supplementary motor area: an event-related fMRI study. Brain Res. Cogn. Brain Res. 21, 206–215.

Mann, D.M.A., Yates, P.O., 1979. The effects of ageing on the pigmented nerve cells of the human locus caeruleous and substantia nigra. Acta Neuropathol. 47, 93–97.

Mark, R.E., Rugg, M.D., 1998. Age effects on brain activity associated with episodic memory retrieval. An electrophysiological study. Brain 121, 861–873.

Mattay, V.S., Callicott, J.H., Bertolino, A., Santha, A.K.S., van Horn, J.D., Tallent, K.A., Frank, J.A., Weinberger, D.R., 1998. Hemispheric control of motor function: a whole brain echo planar fMRI study. Psychiatry Res. 83, 7–22.

Mattay, V.S., Fera, F., Tessitore, A., Hariri, A.R., Das, S., Callicott, J.H., Weinberger, D.R., 2002. Neurophysiological correlates of age-related changes in human motor function. Neurology 58, 630–635.

McIntosh, A.R., Gonzalez-Lima, F., 1994. Structural equation modeling and its application to network analysis in functional brain imaging. Hum. Brain Mapp. 2, 2–22.

McIntosh, A.R., Grady, C.L., Ungereider, L.G., Haxby, J.V., Rapoport, S.I., Horwitz, B., 1994. Network analysis of cortical visual pathways mapped with PET. J. Neurosci. 14, 655–666.

Middleton, F.A., Strick, P.L., 2000. Basal ganglia and cerebellar loops: motor and cognitive circuits. Brain Res. Rev. 31, 236–250.

Muakkassa, K.F., Strick, P.L., 1979. Frontal lobe inputs to primate motor cortex: evidence for four somatotopically organized 'premotor areas'. Brain Res. 177, 176–182.

Naccarato, M., Calautti, C., Jones, P.S., Day, D.J., Carpenter, T.A., Baron, J.-C., 2006. Does healthy aging affect the hemispheric activation balance during paced index-to-thumb opposition task? An fMRI study. NeuroImage 32, 1250–1256.

O'Boyle, D.J., Freeman, J.S., Cody, F.W.J., 1996. The accuracy and precision of timing of self-paced, repetitive movements in subjects with Parkinson's disease. Brain 119, 51–70.

Oldfield, R.C., 1971. The assessment and analysis of handedness: the Edinburgh inventory. Neuropsychologia 9, 97–113.

Park, H.L., O'Connell, J.E., Thomson, R.G., 2003. A systematic review of cognitive decline in the general elderly population. Int. J. Geriatr. Psychiatry 18, 1121–1134.

Pastor, M.A., Jahanshahi, M., Artieda, J., Obeso, J.A., 1992. Performance of repetitive wrist movements in Parkinson's disease. Brain 115, 875–891.

Pastor, M.A., Day, B.L., Macaluso, E., Friston, K.J., Frackowiak, R.S.J., 2004. The functional neuroanatomy of temporal discrimination. J. Neurosci. 24, 2585–2591.

Riecker, A., Groschel, K., Ackermann, H., Steinbrink, C., Witte, O., Kastrup, A., 2006. Functional significance of age-related differences in motor activation patterns. NeuroImage 32, 1345–1354.

Rizzolatti, G., Luppino, G., Matelli, M., 1998. The organization of the cortical motor system: new concepts. Electroencephalogr. Clin. Neurophysiol. 106, 283–296.

Rouiller, E.M., Babalian, A., Kazennikov, O., Moret, V., Yu, X.M., Wiesendanger, M., 1994. Transcallosal connections of the distal forelimb representations of the primary and supplementary motor cortical areas in macaque monkeys. Exp. Brain Res. 102, 227–243.

Rowe, J., Stephan, K.E., Friston, K., Frackowiak, R.S., Lees, A., Passingham, R., 2002. Attention to action in Parkinson's disease: impaired effective connectivity among frontal cortical regions. Brain 125, 276–289.

Rowe, J.B., Siebner, H., Filipovic, S.R., Cordivari, C., Gerschlager, W., Rothwell, J., Frackowiak, R., 2006. Aging is associated with contrasting changes in local and distant cortical connectivity in the human motor system. NeuroImage 32, 747–760.

Sailer, A., Dichgans, J., Gerloff, C., 2000. The influence of normal aging on the cortical processing of a simple motor task. Neurology 55, 979–985.

Shima, K., Tanji, J., 1998. Both supplementary and presupplementary motor areas are crucial for the temporal organization of multiple movements. J. Neurophysiol. 80, 3247–3260.

Smith, C.D., Umberger, G.H., Manning, E.L., Slevin, J.T., Wekstein, D.R., Schnitt, F.A., Markesbery, W.R., Zhang, Z., Gerhardt, G.A., Kryscio, R.J., Gash, D.M., 1999. Critical decline in fine motor hand movements in human aging. Neurology 53, 1458–1461.

Taniwaki, T., Okayama, A., Yoshiura, T., Nakamura, Y., Goto, Y., Kira, J., Tobimatsu, S., 2003. Reappraisal of the motor role of basal ganglia: a functional magnetic resonance image study. J. Neurosci. 23, 3432–3438.

Taniwaki, T., Okayama, A., Yoshiura, T., Togao, O., Nakamura, Y., Yamasaki, T., Ogata, K., Shigeto, K., Ohyagi, Y., Kira, J., Tobimatsu, S., 2006. Functional network of the basal ganglia and cerebellar motor loops in vivo: different activation patterns between self-initiated and externally triggered movements. NeuroImage 31, 745–753.

Tanji, J., Shima, K., 1994. Role of supplementary motor area cells in planning several movements ahead. Nature 371, 413–416.

Vakil, E., Kahan, S., Huberman, M., Osimani, A., 2000. Motor and non-motor sequence learning in patients with basal ganglia lesions: the case of serial reaction time (SRT). Neuropsychologia 38, 1–10.

Volkow, N.D., Gur, R.C., Wang, G.J., Fowler, J.S., Moberg, P.J., Ding, Y.S., Hitzemann, R., Smith, G., Logan, J., 1998. Association between decline in brain dopamine activity with age and cognitive and motor impairment in healthy individuals. Am. J. Psychiatry 155, 344–349.

Ward, N.S., Frackowiak, R.S.J., 2003. Age-related changes in the neural correlates of motor performance. Brain 126, 873–888.

Welford, A.T., 1988. Reaction time, speed of performance, and age. Ann. N. Y. Acad. Sci. 515, 1–17.

Wu, T., Hallett, M., 2005. The influence of normal human ageing on automatic movements. J. Physiol. 562, 605–615.

■臨床経験

退行期うつ病で長期入院中に発症した孤発性Creutzfeldt-Jakob病

前川　敏彦[1]　佐々木健介[2]　安岡　克倫[3]
田北　昌史[4]　門司　晃[1]　神庭　重信[1]

抄録：Creutzfeldt-Jakob病（CJD）は，プリオン病群の一病型として認知症・ミオクローヌス・周期性同期性放電（PSD）を3主徴とする稀な神経変性疾患と思われてきたが，牛肉から感染した変異型CJDの発生などでプリオン病は社会的な注目を集めている。孤発性CJDの前駆症状はうつ病の症状と重なる部分も多く，実際に前駆期には診断を誤ることもある。今回われわれは退行期うつ病として診断され，精神科病院に長期入院中に発症した孤発性CJDを経験した。症例は68歳男性，元来は健康であった。63歳時に退行期うつ病と診断されて，精神科病院に入院し，いったんうつ病は軽快したもののその後CJDを併発した。発症後は典型的な経過をたどり，剖検所見などから診断確定例と診断した。発症早期には脳波所見，髄液検査所見，拡散強調MRI画像が有用であった。発症5年前にうつ病エピソードがあり，CJD前駆期の活動性低下と過去のうつ病の再燃との鑑別が困難であった。早期の鑑別診断のためにCJDの抑うつ症状評価について今後さらに症例を重ねて検討する必要があると考えられた。

精神科治療学　22(11)；1313-1318，2007

Key words：*Creutzfeldt-Jakob disease, depression, prion, differential diagnosis*

Ⅰ．はじめに

初老期に進行性認知症をきたすCreutzfeldt-Jacob病（CJD）は，異常プリオン蛋白が検出されるプリオン病群の一病型として認知症・ミオクローヌス・周期性同期性放電（periodic synchronous discharge：PSD）を3主徴とする，稀な神経変性疾患と思われてきた。近年では市販の脳硬膜製品による感染[7]や牛肉からの感染[11]などでプリオン病は社会的な注目を集めている。あるいはまた，遺伝病としての側面の報告もあり[3]，病原体や発生機序についてはいまだ不明ながら，感染病と遺伝病の両者の特徴を有する疾患群と考えられ

2007年8月29日受理
A case of sporadic Creutzfeldt-Jakob disease during long stay in psychiatric hospital because of senile depression.

[1]九州大学大学院医学研究院精神病態医学
〔〒812-8582　福岡市東区馬出3-1-1〕
Toshihiko Maekawa, M.D., Ph.D., Akira Monji, M.D., Ph.D., Shigenobu Kanba, M.D., Ph.D.: Department of Neuropsychiatry, Graduate School of Medical Sciences, Kyushu University. 3-1-1, Maidashi, Higashi-ku, Fukuoka-shi, Fukuoka, 812-8582 Japan.

[2]九州大学大学院医学研究院神経病理学
Kensuke Sasaki, M.D., Ph.D.: Department of Neuropathology, Graduate School of Medical Sciences, Kyushu University.

[3]高知ハーモニー・ホスピタル
Katsunori Yasuoka, M.D., Ph.D.: Kochi Harmony Hospital.

[4]今津赤十字病院
Masashi Takita, M.D., Ph.D.: Imazu Red Cross Hospital.

る。

孤発性CJD前駆症状は食欲不振，頭痛，倦怠感，睡眠障害，体重減少，不安感など，うつ病と重なる部分も多く，実際に前駆期には診断を誤ることもある[1]。近年プリオン病に対する治療薬の臨床試験が試みられており[10]，今後はさらにできるだけ早期に鑑別診断を行うことが必要である。今回われわれは退行期うつ病として診断され，精神科病院入院中に孤発性CJDを発症し，うつ病の再燃と鑑別が困難であった症例を経験したので報告する。

Ⅱ．症　　例

家族歴：8人同胞の7番目。2人の兄と1人の弟が脳出血，姉が脳梗塞で死亡した。

既往歴：63歳時に胃潰瘍

生活歴・現病歴：元来融通の利かない性格であった。高卒後，4年間公務員を務めた。その間に大型自動車免許を取得し，トラック運転手に転職後，停年（58歳）まで勤務した。社宅で生活し人付き合いはほとんどせず結婚もしなかった。退職後は公営住宅に一人で住みパチンコばかりに行き退職金をほとんど浪費し，63歳頃からこのような生活を続けていてはいけないと考え込むようになった。次第に気分が落ち込み，不眠，食欲不振となり，自ら近医内科を受診した。胃潰瘍と診断されて10日入院し，胃潰瘍は治癒したものの抑うつ気分，不眠，食欲不振は遷延していた。退院3日後，焦燥感が高まり，自ら隣人に救急車を呼んでもらい，救急病院に搬送されたが，内科検査で異常なく精神科病院に同日入院した。入院時現症では，意思疎通は良好であったが，抑うつ気分，不眠，食欲低下に加えて焦燥感が強く，全く落ち着かない状態であった。退行期うつ病と診断されてsulpiride 150mg/日，haloperidol 2.25mg/日を投与された。その後，次第に症状が増悪し，拒食，拒薬，無言，臥床の亜昏迷状態となったが，経管栄養などして半年ほどで徐々に回復した。入院15ヵ月後には，fluvoxamineに主剤を変更したところ，さらに抑うつ気分は改善され，日常生活面での活動性も向上した。その頃には治療面接では理路整然とスムースに応答し抑うつ気分などは感じられず，病棟内の配膳準備や清掃などの手伝いなどを率先して行っていた。しかし，経済的には姉が入院費を支払っている状態で本人の社会復帰の意欲が低下していたので退院できず，いわゆる社会的入院が続いていた。X年12月頃（68歳）より急に活動性が低下し，他患と交流せず自室で過ごす時間が目立って多くなった。当時の主治医は普段の様子と比べて元気のない印象は受けたが，うつ病の再燃を考慮しながら特に血液検査などすることなく様子を観察していた。約1ヵ月後のX＋1年1月20日より歩行困難，動作緩慢となった。X＋1年2月13日脳波ではPSDを示唆する初期所見，頭部拡散強調MRIでは右尾状核，右大脳皮質に広汎に高信号域を認めた。返答の遅れ，記銘力低下がみられ，2月13日頃までは意思疎通可能だったが次第に疎通が取れなくなった。ADLも急激に低下し，2月16日より尿便失禁，咀嚼・嚥下不能となり流動食を開始した。2月20日頃には上半身がベッドより落ち，両上下肢をガクガクと動かして，尿失禁がみられた。時折，部分的に四肢の振戦がみられ，外界の刺激に反応しミオクローヌス様けいれんが全身に及んだ。次第にけいれんの頻度が増し間歇的に全身けいれんを引き起こし，体位変換時外力の刺激によりけいれんが必発した。3月に入る頃には完全に疎通はとれず重度認知症状態となり，その後は呼吸器・尿路感染を繰り返し，X＋2年4月死亡した。臨床症状経過と画像経過をそれぞれ図1，図2に示す。

Ⅲ．検 査 所 見

髄液検査：リンパ球3/12，neuron specific enolase（NSE）146，14-3-3蛋白（＋＋），プリオン蛋白遺伝子：codon129 Met/Met, codon219 Glu/Glu，脳波検査（図3）：全般性のPSD，頭部CT（図2）：びまん性脳萎縮，頭部MRI（図2）：T2強調画像；びまん性脳萎縮，両側大脳基底核にT2延長，拡散強調画像；大脳基底核に拡散係数（apparent diffusion coefficient：ADC）低下を伴う異常信号，頭部Tc-99m SPECT（図2）：両側前頭・側頭・頭頂葉と左線条体血流低下。

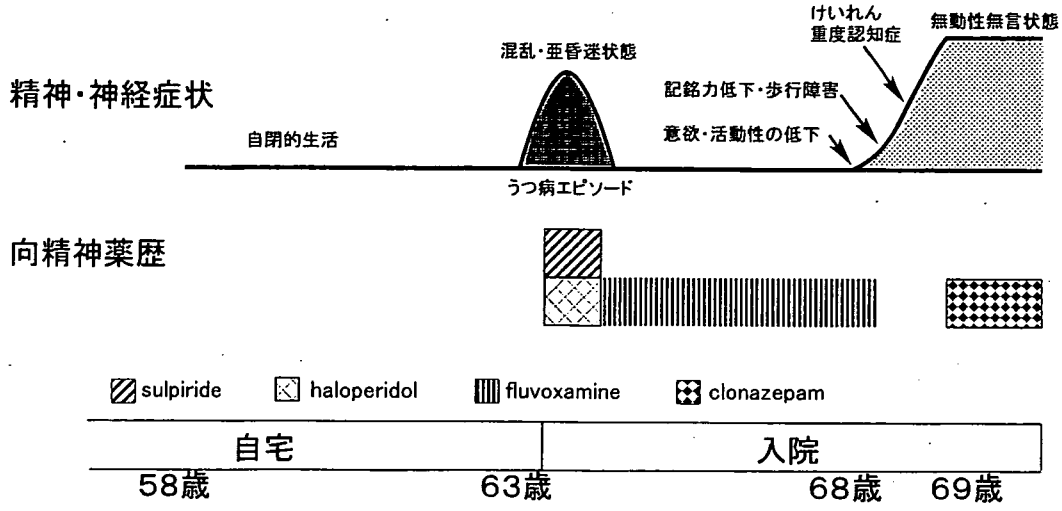

図1　うつ病発症前からCJD発症後死亡までの臨床経過
CJD発症前に約5年間うつ病として精神科病院に入院していたが，うつ病とCJDの因果関係は不明である。

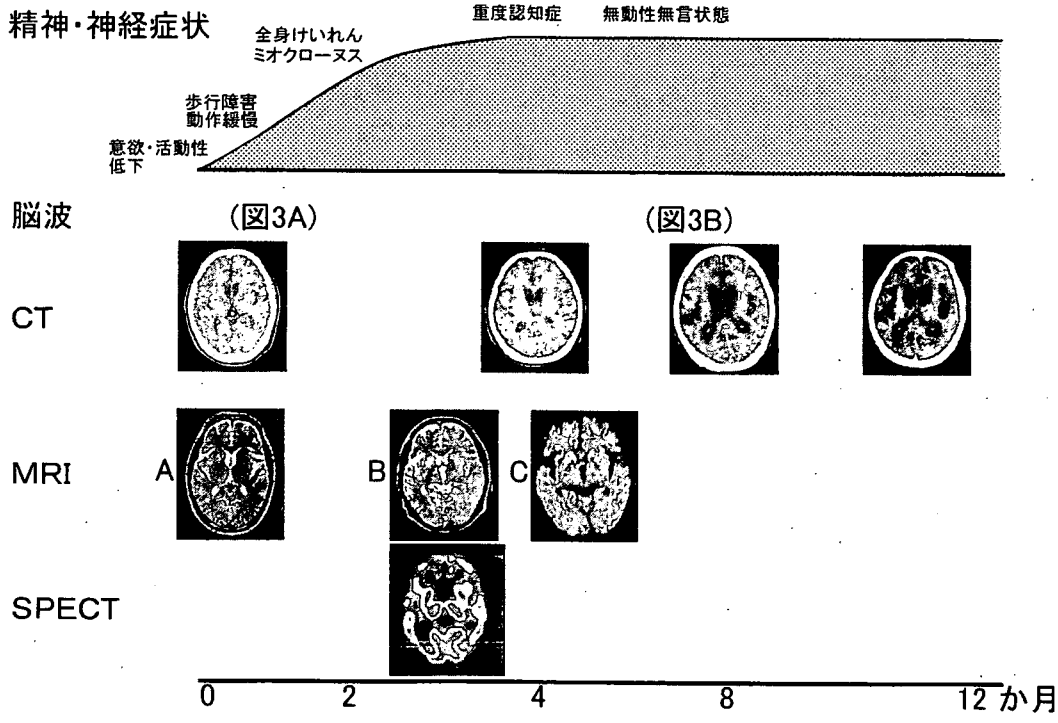

図2　CJD発症後臨床経過と画像検査所見
CJD発症後は典型的な臨床経過をたどって約15ヵ月後呼吸器・尿路感染によって死亡した。CT検査では初期には異常は目立たなかったが，急激にびまん性脳萎縮が進行した。発症2.5ヵ月後のMRI画像では，A（T2強調画像，発症1.5ヵ月後）：びまん性脳萎縮，両側大脳基底核に淡いT2延長を認める。B（T2強調画像，発症2.5ヵ月後）：びまん性脳萎縮，両側大脳基底核にT2延長を認めた。C（拡散強調画像，発症2.5ヵ月後）：大脳基底核にADC低下を伴う異常信号を認めた。Tc-99m SPECT検査（発症3ヵ月後）では，両側前頭・側頭・頭頂葉および左線条体の血流低下を認めた。紙面の都合上，脳波所見は図3に示すが，初期には脳波の基礎律動の徐波化，髄液14-3-3蛋白の高値と拡散強調MRI画像のADC低下を含む異常信号が診断に有用であった。

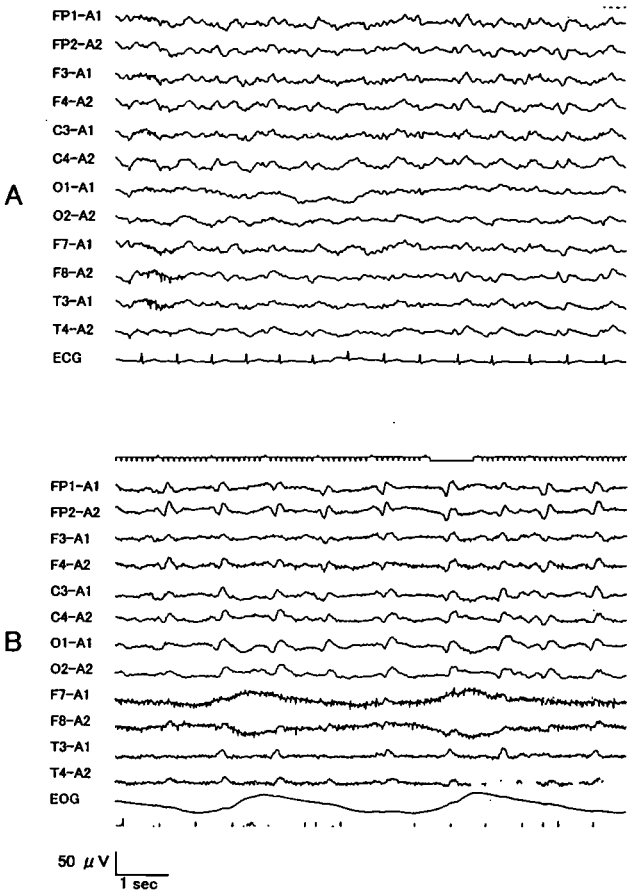

図3　CJD発症後の脳波の経過

A：発症1.5ヵ月後。優位律動が消失しており，全般性に不規則2～3 Hzδ波が持続し，間欠的に前方優位8～9 Hzの律動波が重畳する。一部は周期的に鋭波様の活動がみえる部分もある。B：発症約7ヵ月後。前回の脳波より背景は単調になっており，両側同期性周期性に高振幅鋭波（PSD）が出現している。

Ⅳ．剖検所見

脳重量940gで高度脳萎縮。大脳皮質を中心に高度な粗鬆化，神経細胞脱落，グリオーシスを認めた。海馬は比較的病変が軽度で典型的な海綿状変化が確認された。その他，視床背内側核群，被殻，小脳顆粒細胞層で高度な神経細胞脱落，グリオーシスを認めた。プリオン蛋白免疫染色にて，異常なシナプス型の染色が確認された。ウエスタンブロッティングにても同様にプロテアーゼ抵抗性異常型プリオン蛋白（type1）が確認された。

Ⅴ．考　察

退行期うつ病と診断されて入院5年後に発症した孤発性CJD症例である。発症後の臨床症状，経過，検査所見，剖検所見から典型的な古典的CJDと判断された。本症例の特徴は発症5年前にうつ病エピソードがあり，その後退院することなく入院継続中に発症し，急速進行した点である。以下に古典的CJDの一般的な経過[6]と比較しながら本症例の経過を考察した。

1．古典的CJDの一般的な経過

厚生労働省研究班マニュアル[6]によれば，古典的CJDの有病率は100万人に1人前後であり，地域差はない。発症年齢は平均63.0歳（標準偏差10.4，レンジ25～85歳）である。臨床症状は，発症前に食欲不振，頭痛，倦怠感，睡眠障害，体重減少，あるいは不安感などが1～2ヵ月みられることがある。発症後は精神・高次機能障害で始まり急速に進行し，褥瘡，誤嚥性肺炎，尿路感染症などを併発して1～18ヵ月（平均3.9ヵ月）で死亡するが，数年にわたる症例もある。また，血算，血清生化学，免疫，炎症の検査，尿には異常を認めない。脳波は発症初期には基礎律動の不規則化と徐波化がみられるが，ミオクローヌスが出現する時期にはPSDがみられるようになる。末期になるとPSDが消失して脳波は平坦化する。髄液では軽度の蛋白増加を認めることがあるが，細胞数は正常である。早期にNSE，および14-3-3蛋白の増加が認められ，診断的価値が高い[12]。画像検査では，MRIが初期診断には有用である。FRAIR法や拡散強調MRIでは，基底核，視床や大脳皮質に沿って異常な高信号が高率に見出される。鑑別診断には，老年期認知症性疾患が挙げられるが，CJDでは認知症，ミオクローヌス，脳波検査でのPSDの3徴候に加え，無言性無動に至る経過が早いこと，画像では全脳の萎縮が急速に進行すること，髄液での14-3-3蛋白の陽性が診断上重要である。剖検所見では，著明な脳萎縮があり，重量は1,000g以下であることが多い。割面で灰白質，白質ともに萎縮，変色し，脳室は拡大す

る。海綿状態がのちに粗鬆化やstatus spongiosusに代わり，大脳皮質や基底核を中心に認められる。免疫染色によって異常プリオン蛋白が灰白質にびまん性に染色される。

2．本症例の特徴

以上の古典的CJDの知見から本症例は，発症後は典型的な経過をたどった診断確定例と診断した。本症例でX年12月よりみられた活動性の低下は現時点から振り返るとCJD前駆期の精神症状であった可能性が推測される。しかし，当時の主治医は過去のうつ病エピソードの再燃を考慮して経過観察にとどめてCJDに必要な初期検査が遅れた。以前にも仮性認知症と誤診[1]，アルツハイマー病との鑑別困難[9]あるいは合併[5]，今回のようにうつ病との鑑別困難[4]などの症例が報告されている。いずれの症例もCJD前駆期の症状評価は初期診断の症状との鑑別が困難であったことが推測され，病初期に感度が比較的よいとされている，脳波検査，MRI検査（拡散強調），髄液検査すべては行えていない。

Bernoulliら[2]は100例のCJDについて初期症状を分析して3期に分類している。そのうちでも最も早期の第1期では「身体的ないし精神的な異常の自覚はあるが，日常生活に支障をきたすほどではない。軽度の（“微細な”）感覚運動兆候や行動兆候はあってもなくてもよい」と定義している。彼らによると，第1期の症状では精神障害・人格変化・行動異常が50例にみられ，もっとも多かったのは抑うつ，または不安で17例であった。また第1期の持続期間は平均9週間で1～52週間に分布していた。この記述は本症例ではうつ病エピソードのあった入院時ではなく，X年12月をCJDの発症とすることを支持している。一方，小林ら[4]，酒向ら[8]が考察しているように，CJD前駆症状の精神症状に抗うつ薬や抗精神病薬は効果がないというエビデンスはなく，彼らの症例では以前から脳波あるいはSPECTで異常があったことから発症1年以上前から存在する抑うつ気分をCJDと関連付けることも否定はできない。しかし，本症例も含めてCJD前駆期には精神症状だけからその他の初期診断との鑑別は困難であり，CJD発症前の症状を詳しく記載して症例を重ねていくしかないように思える。本症例の精神症状の特徴は，入院前は抑うつ感とともに焦燥感の高まりを訴えていたのに対して，CJD発症直前は「急に活動性が低下し，他患と交流せず自室で過ごす時間が目立って多くなった」として表現されていたことである。孤発性CJDの前駆症状では脳の破壊に伴った刺激症状とも言える，ぴりぴりした感じを見受けることもあるが，本症例のように焦燥感を認めず，活動性の低下が目立つ症例も存在する[6]。また，本症例の場合の活動性低下は日時が他者から大体わかるほど急性に出現することも特徴的である。本症例での反省点は入院時点で，うつ病以外の器質的な疾患も考慮して脳波検査や頭部MRI検査などを施行しておくべきだったことである。

Ⅵ．結　語

退行期うつ病で精神科病院に長期入院中に発症した孤発性Creutzfeldt-Jakob病を報告した。うつ病が先行するCJD症例は2，3報告があるが因果関係ははっきりしていない。早期鑑別診断のためにCJD前駆期の抑うつ症状の特徴を今後さらに症例を重ねて検討する必要があると思われた。

本症例は，第102回日本精神神経学会総会（福岡市，2006年）にて発表した。

謝　辞

貴重な資料を提供いただいた行橋記念病院・一甲則男院長に深謝いたします。

文　献

1) Azorin, J.M., Donne, A., Dassa, D. et al.: Creutzfeldt-Jakob disease misdiagnosed as depressive pseudodementia. Comprehens. Psychiatry, 34; 42-44, 1993.
2) Bernoulli, C.Ch., Masters, C.L., Gajdusek, D.C. et al.: Early clinical features of Creutzfeldt-Jakob disease (subacute spongiform encephalopathy). In: (eds.), Prusiner, S.B. and Hadlow, W.J. Slow Transmissible Diseases of the Nervous System: volume I. Academic Press, New York, p.229,

1979.
3) Inoue, L, Kitamoto, T., Doh-ura, K. et al.: Japanese family with Creutzfeldt-Jakob disease with codon 200 point mutation of the prion protein gene. Neurology, 44; 299-301, 1994.
4) 小林聡幸, 青沼架佐賜, 塩原順子ほか: 遷延性抑うつ状態が先行したCreutzfeldt-Jakob病の1剖検例. 精神医学, 37; 1177-1183, 1995.
5) 古賀寛, 納富昭人, 清田正ほか: アルツハイマー型痴呆にクロイツフェルト-ヤコブ病が合併した症例. 老年精神医学雑誌, 4; 183-189, 1993.
6) 厚生労働省特定疾患対策研究事業:「遅発性ウイルス感染調査研究班」クロイツフェルト・ヤコブ病診療マニュアル〔改訂版〕, 2002年1月.
7) 厚生省調査研究:「クロイツフェルト・ヤコブ病等に関する緊急全国調査研究班」研究報告書（班長: 佐藤猛), 1997年3月.
8) 酒向究, 伊藤徹, 大原貢ほか: 抑うつ状態が初発症状に見られ経過中に慢性硬膜下血腫を合併したCreutzfeldt-Jakob病の1例. 臨床精神医学, 21; 891, 1992.
9) 佐藤正剛, 川島敏郎, 要斉ほか: 病初期にAlzheimer病との鑑別が困難であった孤発性Creutzfeldt-Jakob病の一剖検例. 九州精神神経医学, 43; 42-50, 1998.
10) 坪井義夫, 山田達夫, 堂浦克美: プリオン病の治療—ペントサンポリサルフェート脳室内持続投与—. 神経内科, 63; 441-445, 2005.
11) Will, R.G., Ironside, J.W., Zeidler, M. et al.: A new variant of Creudtzfeldt-Jakob disease in the UK. Lancet, 356; 999-1000, 2000.
12) Zerr, I., Pocchiari, M., Collins, S. et al.: Analysis of EEG and CSF 14-3-3 protein as aid to the diagnosis of Creutzfeldt-Jakob disease. Neurology, 55; 811-815, 2000.

Available online at www.sciencedirect.com
ScienceDirect
Journal of Psychiatric Research 41 (2007) 763–775
JOURNAL OF PSYCHIATRIC RESEARCH
www.elsevier.com/locate/jpsychires

Genetic structure of the dopamine receptor D4 gene (*DRD4*) and lack of association with schizophrenia in Japanese patients

Hiroshi Mitsuyasu [a], Hiroaki Kawasaki [a,*], Hideaki Ninomiya [b], Naoko Kinukawa [c], Takeharu Yamanaka [d], Tomoko Tahira [e], Vincent P. Stanton Jr. [f], Gregory M. Springett [g], Kenshi Hayashi [e], Nobutada Tashiro [a], Shigenobu Kanba [a]

[a] *Department of Neuropsychiatry, Graduate School of Medical Sciences, Kyushu University, 3-1-1, Maidashi, Higashi-Ku, Fukuoka 812-8582, Japan*
[b] *Fukuoka Prefetural Dazaifu Hospital, Psychiatric Center, 3-8-1, Gojoh, Dazaifu, Fukuoka 818-0125, Japan*
[c] *Department of Medical Information, Graduate School of Medical Sciences, Kyushu University, 3-1-1, Maidashi, Higashi-Ku, Fukuoka 812-8582, Japan*
[d] *Institute for Clinical Research, National Kyushu Cancer Center, 3-1-1, Notame, Minami-Ku, Fukuoka 811-1395, Japan*
[e] *Division of Genome Analysis, Research Center for Genetic Information, Medical Institute of Bioregulation, Kyushu University, 3-1-1, Maidashi, Higashi-Ku, Fukuoka 812-8582, Japan*
[f] *Genome Science Division, RCAST, Tokyo University, 4-6-1, Komaba, Meguro-Ku, Tokyo, 153-8904, Japan*
[g] *Drug Discovery Program, Department of Interdisciplinary Oncology, H. Lee Moffitt Cancer Center, Tampa, FL 33612, USA*

Received 13 September 2005; received in revised form 24 May 2006; accepted 30 May 2006

Abstract

In order to investigate the contribution of genetic variation in the human dopamine receptor D4 gene (*DRD4*) to the risk of developing schizophrenia, we carried out a genetic analysis of 27 polymorphisms in 216 schizophrenic patients and 243 healthy controls from the Kyushu region of Japan. Twenty-two single nucleotide polymorphisms (SNPs) and five insertion/deletion polymorphisms were analyzed in this study, including four novel SNPs and a novel mononucleotide repeat. Linkage disequilibrium (LD) and haplotype analyses reveal weak LD across the *DRD4* gene. In univariate analysis female individuals with allele −521C had a higher risk for schizophrenia. However, this finding was not significant after correction for multiple hypothesis testing. No other polymorphisms or haplotypes differed between schizophrenic patients and controls. Likewise, multivariate analyses did not reveal any statistically significant associations.

Keywords: Schizophrenia; Genetic association; Polymorphism; Dopamine receptor D4; Linkage disequilibrium; Haplotype

1. Introduction

Schizophrenia is the most prevalent of the major psychotic disorders with 1% of the population affected worldwide. Although family, twin and adoption studies strongly suggest that genetic variation contributes to the etiology of schizophrenia (Gottesman, 1991; Kendler and Diehl, 1993), the underlying molecular basis and pathophysiological mechanisms leading to the development of schizophrenia are still unclear. Several lines of clinical and pharmacological evidence suggest the possible involvement of dopaminergic neurotransmission systems in the pathogenesis of schizophrenia (reviewed by Willner, 1997). The "dopamine hypothesis" is supported by the observation that dopamine receptor antagonists modulate the symptoms of schizophrenia and the observation of altered dopamine levels in the striatum, prefrontal cortex and limbic system of schizophrenic patients. Accordingly dopamine receptors have been a focus of genetic studies aimed at finding abnormalities associated with schizophrenia. In particular, the *DRD4* gene, a member of the D2-like dopamine receptor family, has been considered a strong candidate gene for schizophrenia. This is partly based on the finding that the atypical antipsychotic drug, clozapine, has a relatively high affinity for DRD4 (Van Tol et al., 1991), and

* Corresponding author. Tel.: +81 92 642 5626; fax: +81 92 642 5644.
E-mail address: hiroakik@npsych.med.kyushu-u.ac.jp (H. Kawasaki).

0022-3956/$ - see front matter © 2006 Elsevier Ltd. All rights reserved.
doi:10.1016/j.jpsychires.2006.05.014

that elevated levels of DRD4 protein and mRNA were found postmortem in the brains of schizophrenia patients (Seeman et al., 1993; Stefanis et al., 1998). The DRD4 gene has also been investigated in attention deficit hyperactivity disorder (ADHD) and in relation to personality traits such as novelty seeking.

The *DRD4* locus is highly polymorphic (Cichon et al., 1995; Mitsuyasu et al., 2001; Mitsuyasu et al., 1999; Okuyama et al., 2000; Paterson et al., 1996; Seaman et al., 1999; Van Tol et al., 1992; Wang et al., 2004; Wong et al., 2000).

Association between various polymorphisms and schizophrenia have been reported by some investigators, however, efforts to replicate those results have generally been unsuccessful. Only three studies reported positive association results (Okuyama et al., 1999; Weiss et al., 1996; Xing et al., 2003). Among the polymorphisms analyzed for association with schizophrenia, the −521T/C polymorphism is one of the most extensively studied, not only in relation to schizophrenia (Jonsson et al., 2001; Jonsson et al., 2003; Mitsuyasu et al., 2001; Okuyama et al., 1999; Xing et al., 2003), but also ADHD (Bellgrove et al., 2005; Kirley et al., 2004; Lowe et al., 2004; Mill et al., 2003) and personality traits (Bookman et al., 2002; Ekelund et al., 2001; Joyce et al., 2003; Lakatos et al., 2002; Lee et al., 2003; Mitsuyasu et al., 2001; Okuyama et al., 2000; Ronai et al., 2001; Strobel et al., 2002; Strobel et al., 2003). However, although several studies suggest that the 48-base pair (bp) variable number of tandem repeat (VNTR) polymorphism in exon 3 of *DRD4* is associated with ADHD and personality traits (Faraone et al., 2005; Jonsson et al., 2003; Savitz and Ramesar, 2004; Schinka et al., 2002), the overall results of these extensive investigations are inconsistent.

Previously, we reported nine novel polymorphisms in the upstream region of the *DRD4* gene in the Japanese population (Mitsuyasu et al., 1999). Our analysis of five single nucleotide polymorphisms (SNPs), including −521T/C, in 208 schizophrenia patients and 210 normal controls revealed no significant association (Mitsuyasu et al., 2001).

In this report, we describe a more exhaustive analysis of polymorphism in the *DRD4* gene by carrying out LD and haplotype analyses with a total of 27 polymorphisms including the polymorphic 120-bp tandem repeat (TR) in the 5′ UTR and the 48-bp VNTR in exon 3. Both SNP and haplotype based association analyses, using uni- and multivariate statistical methods, were carried out to clarify the relationship between schizophrenia and polymorphisms of *DRD4*.

2. Materials and methods

2.1. Study population

Two hundred sixteen schizophrenic patients fulfilling the DSM-IV diagnostic criteria for schizophrenia (121 male and 95 female), aged 18–82 (mean 51.5 ± 13.7, male 50.5 ± 14.0, female 52.7 ± 13.3), were recruited from nine hospitals in the northern area of Kyushu. 243 controls (138 male and 105 female), aged 30–71 years (mean 50.2 ± 4.6, male 52.1 ± 1.2, female 47.7 ± 6.1), were recruited from the personnel of the Japanese Self-Defense Forces and the staff of three hospitals in Fukuoka prefecture, Kyushu. All patients and controls were ethnically Japanese. There are no significant differences between the ages of the schizophrenic and control populations, or between male schizophrenics and controls, total female and total male populations or female and male schizophrenic populations. In contrast, there are significant age differences between female and male control populations and between female patients vs. controls: the average female control is 4.3 years younger than the average male control ($p < 0.0001$) and 5.0 years younger than the average female schizophrenic ($p = 0.001$).

The controls were selected based on information acquired from a questionnaire that interrogated various aspects of socio-economic, physical and mental status, as well as neuro-psychiatric and psychological characteristics. This questionnaire provides information similar to that obtained from batteries such as the Temperament and Character Inventory (Cloninger et al., 1993; Kijima et al., 1996), the Beck Depression Inventory (Beck et al., 1961), the State-Trait Anxiety Inventory (Spielberger et al., 1970), the Maudsley Obsessive-Compulsive Inventory (Hodgson and Rachman, 1977), and the Kurihama Alcoholism Screening Test (Saito and Ikegami, 1978). The inclusion criteria for controls were: (1) over 30 years old, (2) no physical or psychiatric history, (3) good social adjustment with occupation, and (4) no intellectual deficit. All control subjects were assessed for mental and physical illness by administering the Japanese edition of the Mini-International Neuropsychiatric Interview (M.I.N.I.) (Sheehan and Lecrubier, 1998).

All subjects gave informed consent. This study was approved by and performed in accordance with the guidelines of the Ethics Committee of the Graduate School of Medical Sciences, Kyushu University.

2.2. Genotyping methods

Genomic DNA was purified from peripheral blood leukocytes as previously described (Lahiri and Nurnberger, 1991; Mitsuyasu et al., 2001). Genotyping experiments were performed using polymerase chain reaction (PCR) and/or direct sequencing methods. The amplified fragments and primer pairs for PCR are summarized in Table 1 and Fig. 1. Both the 120-bp TR and 48-bp VNTR polymorphisms were genotyped by detecting the length of each amplified fragment. The 26 other polymorphisms were genotyped by sequencing two PCR amplified fragments.

The 120-bp TR polymorphism was genotyped using a previously reported PCR-based typing method (Seaman et al., 1999). Genotypes were read based on the presence of 429-bp and/or 549-bp fragments.